



HAL
open science

Mercury concentrations and stable isotope ratios ($\delta^{13}\text{C}$ and $\delta^{15}\text{N}$) in pelagic nekton assemblages of the south-western Indian Ocean

Pavane Annasawmy, David Point, Evgeny Romanov, Nathalie Bodin

► **To cite this version:**

Pavane Annasawmy, David Point, Evgeny Romanov, Nathalie Bodin. Mercury concentrations and stable isotope ratios ($\delta^{13}\text{C}$ and $\delta^{15}\text{N}$) in pelagic nekton assemblages of the south-western Indian Ocean. *Marine Pollution Bulletin*, 2022, 174, 113151 [16 p.]. 10.1016/j.marpolbul.2021.113151 . hal-04842449

HAL Id: hal-04842449

<https://ut3-toulouseinp.hal.science/hal-04842449v1>

Submitted on 18 Dec 2024

HAL is a multi-disciplinary open access archive for the deposit and dissemination of scientific research documents, whether they are published or not. The documents may come from teaching and research institutions in France or abroad, or from public or private research centers.

L'archive ouverte pluridisciplinaire **HAL**, est destinée au dépôt et à la diffusion de documents scientifiques de niveau recherche, publiés ou non, émanant des établissements d'enseignement et de recherche français ou étrangers, des laboratoires publics ou privés.



Distributed under a Creative Commons Attribution 4.0 International License

Mercury concentrations and stable isotope ratios ($\delta^{13}\text{C}$ and $\delta^{15}\text{N}$) in pelagic nekton assemblages of the south-western Indian Ocean

Pavane Annasawmy^{1*}, David Point¹, Evgeny Romanov², Nathalie Bodin^{3,4}

¹Géosciences Environnement Toulouse (GET), UMR 5563 CNRS, IRD, UPS, CNES, Observatoire Midi Pyrénées (OMP), 14 avenue Edouard Belin, 31400 Toulouse, France

²CITEB (Centre technique de recherche et de valorisation des milieux aquatiques), 97420 Le Port, Île de la Réunion, France

³Institut de Recherche pour le Développement (IRD), Fishing Port, Victoria, Mahé, Seychelles

⁴Sustainable Ocean Seychelles, BeauBelle, Mahé, Seychelles

*Corresponding author¹: angelee-pavane.annasawmy@ird.fr

1 **Abstract**

2 Mercury (Hg) concentrations and stable isotope values ($\delta^{13}\text{C}$ and $\delta^{15}\text{N}$) were investigated in
3 micronekton collected from La Pérouse and MAD-Ridge seamounts, Reunion Island and the
4 southern Mozambique Channel. Organisms occupying epipelagic habitats showed lower Hg
5 concentrations relative to deeper dwelling benthopelagic ones. Increasing Hg concentrations
6 with increasing body size were recorded in the Mozambique Channel and Reunion Island.
7 Positive relationships were observed between Hg levels and $\delta^{15}\text{N}$ values in pelagic nekton
8 assemblages collected at MAD-Ridge seamount and the southern Mozambique Channel,
9 suggesting biomagnification of Hg. Concentrations of Hg in organisms of the south-western
10 Indian Ocean were within the same range of values. Total Hg concentrations depend on a
11 range of factors linked to habitat range, body size and trophic position of the individuals. To
12 our knowledge, this is the first study investigating the patterns of Hg concentrations in
13 pelagic nekton assemblages from the south-western Indian Ocean.

14

15 **Keywords:** Trophic ecology, Mercury, Seamount, Squid, Crustacean, Fish

16 **1. Introduction**

17 Mercury is a unique trace element, displaying different chemical forms in the environment.
18 Mercury exists in its elemental form (Hg^0) in the atmosphere and as inorganic Hg in oceanic
19 waters, with a fraction being converted into monomethyl mercury (MMHg) or dimethyl
20 mercury (DMHg) at ocean depths in oxygen minimum zones (Mason and Fitzgerald, 1993;
21 Fitzgerald et al., 2007; Choy, 2013). MMHg is known to bioaccumulate and biomagnify
22 along the marine food chain (Monteiro et al., 1996; Lavoie et al., 2013; Chennuri et al.,
23 2020), with predators showing higher concentrations than their main prey items (Bustamante
24 et al., 2006). Biomagnification is the transfer of a chemical from the diet to the consumer,
25 generally leading to higher concentrations of the element with increasing trophic level (Gray,
26 2002) and is thus inferred when a significant positive relationship is detected between the
27 element and $\delta^{15}\text{N}$ values (Cheung and Wang, 2008). The rate at which bioaccumulation and
28 bioconcentration of MMHg occurs in the food web depends on its bioavailability at the base
29 of the food chain, trophic interactions and food web assemblages up to apex marine
30 predators. In many fish, Hg exists in its most stable, but also the most toxic methyl form
31 (Cossa et al., 1990). Almost all Hg (>90%) in top predators is MMHg (Cossa et al., 1990;
32 Bloom, 1992; Houssard et al., 2019). MMHg distribution in pelagic fish tends to mimic
33 oceanic MMHg distribution profiles showing higher burdens in fish foraging at depth
34 compared to epipelagic organisms (Choy, 2013; Blum et al., 2013).

35 In marine pelagic food webs, mesopelagic micronekton typically ranges in size from 2 to 20
36 cm and consists of a large and diverse group of organisms which can be divided into the
37 broad categories crustaceans, squids and fishes (Brodeur and Yamamura, 2005; De Forest
38 and Drazen, 2009). This group assemblage represents a substantial biomass in oceanic waters
39 accounting for more than 3.8-11.8 billion tons of mesopelagic fishes reported worldwide
40 (Irigoien et al., 2014; Proud et al., 2018). Available estimates for cephalopods and

41 crustaceans suggest global biomass of at least 55 million tons for a single group of
42 *Ommastrephid* squids (Nigmatullin, 2004) and approximately 380 million tons of Antarctic
43 krill in the Southern ocean (Atkinson et al., 2009). Micronekton exhibits a diverse range of
44 migration strategies including diel vertical migration over several hundreds of meters from
45 deep (below 400 m) to shallower layers (top 200 m) at dusk and inversely at dawn
46 (Lebourges-Dhaussy et al., 2000; Béhagle et al., 2014; Ariza, 2015; Annasawmy et al., 2018,
47 2019, 2020a), reverse migration (Alverson, 1961; Gjørseter, 1977, 1984; Marchal and
48 Lebourges-Dhaussy, 1996), mid-water migration or non-migration (Annasawmy et al., 2018;
49 2019). Migratory micronekton plays an essential role in the oceanic biological pump by
50 transporting organic carbon from the euphotic zone to deeper parts of the oceans (Hidaka et
51 al., 2001; Ariza et al., 2015; LeMoigne, 2019). Micronekton is also preyed upon by tunas,
52 billfishes, sharks, marine birds and marine mammals (e.g., Guinet et al., 1996; Potier et al.,
53 2007; Lambert et al., 2014; Filmalter et al., 2017; Romanov et al., 2020).

54 While Hg concentrations in pelagic and tropical coastal marine fish were subjected to
55 extensive studies worldwide (e.g., Al-Reasi et al., 2007; Cai et al., 2007; Calatayud et al.,
56 2012; Chen et al., 2014; Bodin et al., 2017; Chouvelon et al., 2017; Afandi et al., 2018;
57 Briand et al., 2018; Le Croizier et al., 2019; Houssard et al., 2019), micronekton organisms
58 have received little consideration to date with only few studies having determined Hg
59 concentrations in micronekton species (Asante et al., 2008, 2010; Kojadinovic et al., 2011;
60 Brewer et al., 2012; Chai et al., 2012; Queirós et al., 2020). This study therefore documented
61 for the first time Hg levels and distribution in different pelagic nekton assemblages
62 displaying contrasted foraging and diel migration strategies from four different study sites
63 located in the south-western Indian Ocean. These sites (La Pérouse and MAD-Ridge
64 seamounts, Reunion Island and the southern Mozambique Channel) exhibit different
65 productivity, mesoscale processes and varied proximity to landmasses (Annasawmy et al.,

66 2019; Vianello et al., 2020), hypothesizing that Hg concentrations and local biogeochemistry
67 would possibly differ spatially and vertically in the water column, which could be transferred
68 into the mesopelagic assemblages.

69 Biomagnification of a chemical along the food web can be investigated using stable isotope
70 analyses (Asante et al., 2008). Stable nitrogen isotopes ($\delta^{15}\text{N}$) show an enrichment of 2 to 4‰
71 at each trophic step and can be used to determine trophic levels and trophic relationships
72 (Vanderklift and Ponsard, 2003; Michener and Kaufman, 2007; Martínez Del Rio et al.,
73 2009). Stable carbon isotopes ($\delta^{13}\text{C}$) show an enrichment of 0.5 to 1‰ per trophic step and
74 can be used to indicate sources of primary production, such as aquatic versus terrestrial,
75 inshore versus offshore, or pelagic versus benthic contributions to food intake (Hobson et al.,
76 1994; Rubenstein and Hobson, 2004). Previous studies have shown positive relationships
77 between $\delta^{13}\text{C}$ and $\delta^{15}\text{N}$ values and concentrations of trace elements in micronekton,
78 suggesting biomagnification of these chemicals (Asante et al., 2008, 2010). Stable isotopes of
79 ^{13}C and ^{15}N were further evaluated, whenever possible, to determine the biomagnification of
80 mercury in pelagic nekton assemblages of the south-western Indian Ocean.

81 The main objectives of this study are to investigate the (1) Hg concentrations in the different
82 pelagic nekton categories (crustaceans, fishes and squids), (2) regional variability in Hg
83 concentrations, (3) Hg concentrations with respect to the habitat ranges and feeding modes of
84 the sampled taxa, (4) influence of body size and $\delta^{13}\text{C}$ and $\delta^{15}\text{N}$ values on Hg concentrations.

85

86 **2. Materials and Methods**

87 2.1 Study sites

88 Pelagic nekton assemblages were sampled during several cruises of the RV *Antea* at the La
89 Pérouse and MAD-Ridge seamounts. For comparison with off-seamount locations, pelagic

90 nekton assemblages were also sampled in proximity to Reunion Island during the IOTA
91 cruise and in the southern Mozambique Channel during the MAD-Ridge cruise. La Pérouse
92 cruise (DOI: 10.17600/16004500) was conducted in September 2016 at the seamount at
93 latitude 19°43'S and longitude 54°10'E. IOTA cruise (DOI: 10.17600/16004600) was
94 conducted in the waters surrounding Reunion Island (within 50 nautical miles) and MAD-
95 Ridge Leg 2 cruise was conducted in December 2016 at the MAD-Ridge seamount (latitude
96 27°28.38'S and longitude 46°15.67'E; DOI: 10.17600/16004900) (Fig. 1a). During the MAD-
97 Ridge cruise, four additional mesopelagic trawls were conducted in the southern
98 Mozambique Channel.

99 The four study sites have been chosen with respect to their contrasting oceanographic natures.
100 While La Pérouse seamount is an isolated pinnacle (Marsac et al., 2020) located in a nutrient-
101 poor gyral system (Jena et al., 2013), MAD-Ridge seamount is part of the Madagascar Ridge
102 and in the pathway of mesoscale eddies driving productivity from the Madagascar continental
103 shelf (Vianello et al., 2020; Noyon et al., 2019). Seasonal phytoplankton blooms (between
104 January and March) may occasionally propagate eastwards from South of Madagascar to
105 about 500 km from Reunion Island (Pinet et al., 2012). Reunion Island may thus occasionally
106 experience higher oceanic productivity compared to La Pérouse seamount (Pinet et al., 2012).
107 The southern Mozambique Channel is a site of high oceanic productivity and mesoscale
108 processes due to the prevalence of mesoscale eddies driving productivity from the African
109 continental shelf into the channel (Tew-Kai and Marsac, 2009).

110 2.2 Sampling of pelagic nekton assemblages

111 Pelagic nekton were sampled with a 40-m long International Young Gadoid Pelagic Trawl,
112 having an 80 mm knotless nylon delta mesh netting at the front tapering, 5 mm at the codend
113 and a mouth opening of ~96 m² during all three cruises. The trawl was towed at a vessel

114 speed of ~2-3 knots at the targeted depths for 60 min at La Pérouse and Reunion Island and
115 30 min at MAD-Ridge and in the Mozambique Channel. During all cruises, the sampling
116 depth was that of the sound scattering layer at that ship position and time of day, with no
117 rigid plan of sampling preselected depths. The trawl depth was monitored with a Scanmar
118 depth sensor during all cruises. To account for the different trawl durations, the volume of
119 water filtered by the net tows was estimated by multiplying the distance travelled by the area
120 of the trawl mouth opening. Ten epi-mesopelagic tows were conducted at the La Pérouse
121 seamount, six at Reunion Island, seventeen at MAD-Ridge seamount, and four in the
122 southern Mozambique Channel.

123 The sampled mesopelagic organisms were sorted on board, divided into four broad categories
124 (gelatinous, crustaceans, cephalopods and fishes) and frozen at -20°C. Only the broad
125 categories crustaceans, fishes and squids were analysed during this study and are listed in
126 Table 1. The identified samples were measured (abdomen and carapace length for
127 crustaceans, dorsal mantle length – DML – for squids, and standard length – SL – for fishes).

128 2.3 Mercury analyses

129 Micronekton samples (muscle tissue taken from abdomen for crustaceans, mantle for squids
130 and dorsal musculature for fishes) were freeze-dried in Christ Alpha 1-4 LSC Freeze Dryers
131 for 48h and ground to a fine homogenous powder using an automatic ball mill RETSCH
132 MM200 at 30 oscillations per second for ~10 minutes. Approximately 10-100 mg of dried
133 samples was measured and total Hg concentrations were determined by combustion, gold
134 trapping and atomic absorption spectrophotometry detection using a Direct Mercury Analyser
135 (DMA-80, Milestone, USA). Two freeze-dried certified biological materials, a lobster
136 hepatopancreas (TORT-3, National Research Council Canada; certified Hg concentration:
137 $0.29 \pm 0.02 \mu\text{g g}^{-1}$ dry weight) and a mussel tissue (SRM 2976, National Institute of

138 Standards and Technology; certified Hg concentration: $61.0 \pm 3.6 \mu\text{g g}^{-1}$ dry weight)
139 reference materials and analyses of blanks were used in each sample batch to establish the
140 analytical quality (i.e. accuracy and reproducibility) of the method. Recovery values for each
141 sample batch were not different from the certified values and their associated uncertainty.
142 Three blanks were analysed at the beginning of each sample batch. The DMA-80 achieves a
143 detection limit of $0.005 \mu\text{g g}^{-1}$ dry weight (Le Croizier et al., 2019). Resulting Hg
144 concentrations in pelagic nekton assemblages are given in $\mu\text{g g}^{-1}$ dry weight (dw).

145 2.4 Analysis of stable isotope ratios and trophic level calculations

146 Since variations in lipid composition may influence $\delta^{13}\text{C}$ and $\delta^{15}\text{N}$ values (Bodin et al., 2009;
147 Ryan et al., 2012), lipids were removed from samples using dichloromethane on an
148 accelerated solvent extraction system (ASE[®], Dionex; Bodin et al., 2009). Approximately
149 400-600 μg of dried and ground samples were weighed and placed in tin capsules and were
150 run through continuous flow on a Thermo Scientific Flash 2000 elemental analyser coupled
151 to a Delta V Plus mass spectrometer at the Pôle de Spectrométrie Océan (Plouzané, France).
152 The samples were combusted in the elemental analyser to separate CO_2 and N_2 gases. A
153 reference gas set was used to determine isotopic ratios by comparison. The isotopic ratios
154 were then expressed in the conventional δ notations as parts per thousand (‰) deviations
155 from the international standards:

$$156 \delta^{13}\text{C} \text{ or } \delta^{15}\text{N} (\text{‰}) = [(R_{\text{sample}}/R_{\text{standard}}) - 1] \times 1000$$

157 where R is the ratio of $^{13}\text{C}/^{12}\text{C}$ or $^{15}\text{N}/^{14}\text{N}$.

158 Measurement errors for both the nitrogen and carbon isotopes were $<0.15\%$. For each sample,
159 the C: N ratio did not exceed 3.5, confirming that lipids were efficiently removed from the
160 samples (Post et al., 2007).

161 The trophic level of each selected taxa was calculated using the following equation, based on
162 Minagawa and Wada (1984) and Post (2002):

$$163 \quad 2.0 + \frac{\delta^{15}\text{N}_i - \delta^{15}\text{N}_{\text{primary consumer}}}{3.2}$$

164 where, $\delta^{15}\text{N}_i$ is the nitrogen isotopic value of any given taxon i , $\delta^{15}\text{N}_{\text{primary consumer}}$ is the
165 nitrogen isotopic value of the baseline at trophic level of 2, and 3.2‰ is the estimated trophic
166 enrichment factor between consumers and their primary prey (Michener and Kaufman, 2007;
167 Vanderklift and Ponsard, 2003). In this study, $\delta^{15}\text{N}_{\text{primary consumer}}$ was estimated from the
168 mean $\delta^{15}\text{N}$ values ($5.31 \pm 0.31\text{‰}$) of six pyrosomes and one salp at La Pérouse seamount and
169 from six salps with mean $\delta^{15}\text{N}$ values of $4.22 \pm 1.01\text{‰}$ at MAD-Ridge (Annasawmy et al.,
170 2020b).

171 2.5 Ecological data of selected species

172 The pelagic nekton organisms were classified into different habitat ranges according to
173 literature (Clarke and Lu, 1975; Percy et al., 1977; Smith and Heemstra, 1986; van der Spoel
174 and Bleeker, 1991; Brodeur and Yamamura, 2005; Hastie et al., 2009; Davison et al., 2015;
175 Romero-Romero et al., 2019). Organisms were classified as being epipelagic (<200 m),
176 mesopelagic (from 200 to 1000 m), bathypelagic (below 1000 m and ~100 m from the
177 seafloor) and benthopelagic (living near the bottom but performing excursions into the
178 pelagic realm) according to definitions of the vertical zonation of the pelagic ocean from Del
179 Giorgio and Duarte (2002) and Sutton (2013). The different taxa were thus classified into the
180 groups Epipelagic-Mesopelagic < Mesopelagic < Mesopelagic-Bathypelagic <
181 Mesobenthopelagic, according to their known habitats described in literature.

182 Organisms were further classified as carnivores (all squids, most mesopelagic fishes except
183 Warming's lanternfish *Ceratoscopelus warmingii*) and omnivores (all crustaceans). Most

184 mesopelagic fishes were classified as carnivores since they were reported to feed on
185 copepods, amphipods, euphausiids and ostracods (Dalpadado and Gjørseter, 1988; Pakhomov
186 et al., 1996; Tanaka et al., 2007; Hudson et al., 2014; Bernal et al., 2015; Carmo et al., 2015;
187 Young et al., 2015), with no herbivorous feeding strategy except *C. warmingii* which has
188 developed an adaptive response to competition in low-productive environment (Robison,
189 1984). Crustaceans were classified as omnivores since they were reported to prey on
190 zooplankton, euphausiids, and copepods and are known for occasional herbivory (Hopkins et
191 al., 1994; Birkley and Gulliksen, 2003; Mauchline, 1959; Foxton and Roe, 1974). For species
192 with unknown diets, the feeding mode was determined based on the feeding habits identified
193 from species within the same genus.

194 2.6 Satellite data acquisition

195 Sea surface chlorophyll (SSC) data at a daily and 4.5 km resolution were downloaded from
196 MODIS (<http://oceancolor.gsfc.nasa.gov>) and were used to calculate 5-day averages to obtain
197 a proxy of surface oceanic primary production for the period from 18/09/2016 to 07/12/2016.
198 Delayed-time mean sea level anomalies (MSLAs) at a daily and 1/4° resolution were
199 produced and distributed by the Copernicus Marine Environment Monitoring Service project
200 (CMEMS) and available at <http://marine.copernicus.eu/>. MSLAs were used to describe the
201 mesoscale eddy field at the time of MAD-Ridge cruise.

202 2.7 Statistical analyses

203 Prior to running statistical tests, assumptions of normality using the Shapiro Wilk's test
204 (Shapiro and Wilk, 1965) and homogeneity of variances using the Bartlett test (Bartlett,
205 1937), were computed in R (v. 3.6.1). To investigate variation in Hg concentrations between
206 broad categories, non-parametric Kruskal-Wallis tests were performed followed by pairwise
207 Wilcoxon rank sum tests. Differences in Hg concentrations of the most common taxa

208 (Sergestidae, Penaeidae, Stomiidae, Gonostomatidae and Myctophidae) across the four
209 sampling sites - La Pérouse, MAD-Ridge, Mozambique Channel and Reunion Island - were
210 investigated using Kruskal-Wallis tests. The latter tests were also conducted to assess the
211 variation in Hg concentrations according to the habitat ranges of the sampled micronekton
212 species. Non-parametric Wilcoxon rank sum tests were carried out to investigate the
213 influence of feeding mode (carnivorous or omnivorous) on Hg concentrations at each of the
214 four sampling sites. Linear regressions were computed to assess the relationships between Hg
215 concentration and micronekton body size. Links between $\delta^{13}\text{C}$ and $\delta^{15}\text{N}$ values of all selected
216 micronekton at the sampling sites La Pérouse, MAD-Ridge and Mozambique Channel were
217 investigated using Kruskal-Wallis tests and pairwise Wilcoxon rank sum tests. Statistical
218 models were further applied to test for the influence of $\delta^{13}\text{C}$ and $\delta^{15}\text{N}$ values on Hg
219 concentrations of the broad categories crustaceans, fishes and squids at La Pérouse, MAD-
220 Ridge and in the Mozambique Channel. Links between stable isotope values and Hg
221 concentrations were not investigated at Reunion Island because stable isotope ratios were not
222 available at this site.

223

224 **3. Results**

225 3.1 Prevailing bathymetry and oceanographic processes at the study sites

226 La Pérouse seamount is located within the Indian South Subtropical Gyre (ISSG) province
227 and MAD-Ridge seamount is located ~1300 km southwards from the Madagascar landmass
228 within the East African Coastal province (EAFR) (Fig. 1a). The La Pérouse seamount summit
229 is 10 km long and reaches ~60 m below the sea surface rising from a seabed at ~5000 m (Fig.
230 1b). MAD-Ridge seamount is 33 km long (North to South) and 22 km wide (East to West).

231 The seamount rises from 1600 m from the ocean floor to a summit depth of ~240 m below
232 the sea surface (Fig. 1c).

233 Mean sea surface chlorophyll concentrations were higher at the MAD-Ridge seamount and
234 the southern Mozambique Channel compared to the La Pérouse seamount and Reunion Island
235 (Fig. 2a). During MAD-Ridge cruise in November 2016, a strong anticyclonic eddy was
236 stationed at MAD-Ridge. A weak anticyclonic eddy was stationed at La Pérouse seamount,
237 whereas Reunion Island was under the influence of a weak cyclonic eddy in November 2016
238 (Fig. 2b). During the La Pérouse cruise in September 2016, a weak cyclonic eddy was
239 stationed at the seamount (Annasawmy et al., 2019).

240 3.2 Pelagic nekton species composition, size variability by sampled area and ecological group

241 A total of 60 pelagic nekton taxa were sampled during this study, including 4 crustaceans, 10
242 squids, and 46 fishes (Table 1). Crustaceans were represented by pelagic caridean, penaeid,
243 and sergestid shrimps. Cephalopods consisted of five families of squids (Enoploteuthidae,
244 Histioteuthidae, Ommastrephidae, Onychoteuthidae, and Pyroteuthidae). Fishes were
245 represented by 11 common pelagic families Carangidae, Diretmidae, Gempylidae,
246 Gonostomatidae, Myctophidae, Neoscopelidae, Scombrolabracidae, Phosichthyidae,
247 Sternoptychidae, Stomiidae, and benthopelagic Priacanthidae. In terms of diversity and
248 biomass, sampling was dominated by Myctophidae (22 species) and Stomiidae (12 species)
249 (Table 1).

250 A total of 256 taxa represented small animals of less than a maximum length of 200 mm.
251 Larger organisms were also collected in the trawl including two large individuals of neon
252 flying squids, *Ommastrephes bartramii* (DML = 364.8 and 489.8 mm) and fishes: Roudi
253 escolar, *Promethichthys prometheus* (n = 2, SL = 235.4 and 365.0 mm) and longfinned
254 bullseye, *Cookeolus japonicus* (n = 2, SL range 207.9-328.0 mm). These six specimens

255 represent outliers from the micronektonic community in terms of sizes (neon flying squid and
256 Roudi escolar) and habitat (Roudi escolar and longfinned bullseye) and were hence analysed
257 separately. All calculations of means and medians by broad categories, regions, habitats,
258 feeding modes, sizes and stable isotope values, are presented without taking these species
259 into consideration.

260 The size ranges of fishes were SL 30.8-244.8 mm (mean of 84.9 mm) at La Pérouse, 30.3-
261 289.9 mm (mean of 74.7 mm) at MAD-Ridge seamount, 33.6-371.0 mm (mean of 99.6 mm)
262 in the Mozambique Channel and 18.9-184.9 mm (mean of 121.4 mm) at Reunion Island.
263 Crustaceans showed size ranges of 39.1-84.9 mm (mean of 59.9 mm) at La Pérouse, 33.2-
264 78.5 mm (mean of 56.1 mm) at MAD-Ridge, 55.5-79.2 mm (mean of 69.3 mm) in the
265 Mozambique Channel and 29.5-78.6 mm (mean of 54.2 mm) at Reunion Island. The size
266 ranges of squids were DML 18.3-36.4 mm (mean of 28.3 mm) at La Pérouse, 22.2-163.3 mm
267 (mean of 59.7 mm) at MAD-Ridge and 18.9-81.9 mm (mean of 31.8 mm) at Reunion Island.

268 3.3 Variability in micronekton Hg concentrations

269 Mercury concentrations of all sampled taxa are given in Table 1. No significant differences
270 were observed in Hg concentrations of Gonostomatidae, Myctophidae, Sergestidae,
271 Penaeidae, and Stomiidae between La Pérouse, MAD-Ridge seamounts, the southern
272 Mozambique Channel and Reunion Island (Fig. 3a; Kruskal-Wallis, $p > 0.05$). All
273 micronekton species sampled at Reunion Island showed lower mean Hg concentrations than
274 at La Pérouse and MAD-Ridge seamounts (Kruskal-Wallis, $H= 21.9$, $p < 0.05$) (Fig 3b).
275 Squids exhibited lower median Hg concentrations compared to crustaceans and fishes at La
276 Pérouse, MAD-Ridge and Reunion Island (Kruskal-Wallis, $H= 65.2$, $p < 0.05$; Fig 3c). The
277 two large nektonic neon flying squids collected in the Mozambique Channel and at MAD-
278 Ridge seamount showed high Hg concentrations of $0.92 \mu\text{g g}^{-1} \text{ dw}$ and $0.82 \mu\text{g g}^{-1} \text{ dw}$

279 compared to the other sampled squids (Table 2). At La Pérouse and Reunion Island,
280 Oplophoridae sp. exhibited higher Hg concentrations (1.69 and $1.57 \mu\text{g g}^{-1} \text{dw}$, respectively)
281 than other sampled taxa. The *Funchalia* sp. (Penaeidae) showed lower Hg concentrations
282 (0.05 - $0.06 \mu\text{g g}^{-1} \text{dw}$) than the other crustaceans at MAD-Ridge, the southern Mozambique
283 Channel and Reunion Island. Fishes exhibited higher median Hg concentrations at MAD-
284 Ridge than the other broad categories (with hatchetfish *Argyropelecus aculeatus* showing
285 highest concentrations of $1.12 \mu\text{g g}^{-1} \text{dw}$). The mackerel scad *Decapterus macarellus* showed
286 lower Hg concentrations of $0.03 \mu\text{g g}^{-1} \text{dw}$ among all other sampled fishes at MAD-Ridge
287 seamount, in the southern Mozambique Channel and at Reunion Island (Table 2).

288 Hg concentrations in the sampled micronekton increased from organisms collected near the
289 surface (Epipelagic-Mesopelagic) to deeper parts (Mesopelagic-Benthopelagic) (Kruskal-
290 Wallis, $H=23.8$, $p < 0.05$) (Fig. 3d). Feeding mode (omnivore vs carnivore) of sampled
291 micronekton did not significantly influence Hg concentrations (MAD-Ridge: $W= 685$, $p >$
292 0.05 ; Mozambique Channel: $W= 59$, $p > 0.05$; Reunion Island: $W= 339$, $p > 0.05$), except at
293 La Pérouse seamount ($W= 229$, $p < 0.05$) (Fig. 3e) where omnivorous organisms
294 (representing crustaceans and *C. warmingii* individuals) recorded higher Hg concentrations
295 compared to carnivorous ones. Body size of organisms had a significant positive influence on
296 Hg concentrations in the southern Mozambique Channel ($F_{1, 28} = 18.6$, $p < 0.05$) and at
297 Reunion Island ($F_{1, 74} = 5.14$, $p < 0.05$) with Hg concentrations increasing with micronekton's
298 body size [Mozambique Channel: $Hg(\mu\text{g g}^{-1} \text{dw}) = 0.04 + 0.001 \times \text{Size (mm)}$; Reunion
299 Island: $Hg(\mu\text{g g}^{-1} \text{dw}) = 0.07 + 0.001 \times \text{Size (mm)}$]. No relation was found between Hg
300 concentrations and body size of all micronekton species at the La Pérouse ($F_{1, 58} = 0.006$, $p >$
301 0.05) and MAD-Ridge seamounts ($F_{1, 93} = 0.30$, $p > 0.05$) (Fig 4).

302 3.3 Relationships between Hg concentrations and stable isotope ($\delta^{13}\text{C}$ and $\delta^{15}\text{N}$) values

303 Stable isotope values of $\delta^{13}\text{C}$ and $\delta^{15}\text{N}$ were significantly different between La Pérouse and
304 MAD-Ridge seamounts ($\delta^{13}\text{C}$: Kruskal-Wallis, $H= 16.4$, $p < 0.05$; $\delta^{15}\text{N}$: Kruskal-Wallis, $H=$
305 15.8 , $p < 0.05$), with micronekton showing higher $\delta^{13}\text{C}$ and $\delta^{15}\text{N}$ values at La Pérouse
306 compared to MAD-Ridge (Fig. 5). Micronekton assemblages also exhibited higher $\delta^{13}\text{C}$
307 values at La Pérouse compared to the Mozambique Channel (pairwise comparisons, $p <$
308 0.05). Hg concentrations in the micronekton broad categories were significantly influenced
309 by $\delta^{15}\text{N}$ values at MAD-Ridge ($F_{1, 95} = 18.0$, $p < 0.05$) and in the Mozambique Channel ($F_{1, 28}$
310 $= 10.2$, $p < 0.05$), with an increase in Hg concentrations with increasing $\delta^{15}\text{N}$ values. No
311 significant increase in Hg concentrations with increasing $\delta^{15}\text{N}$ values were observed at La
312 Pérouse ($F_{1, 28} = 1.64$, $p > 0.05$). No clear relationships were found between Hg
313 concentrations and $\delta^{13}\text{C}$ values at the La Pérouse ($F_{1, 28} = 2.37$, $p > 0.05$), MAD-Ridge
314 seamounts ($F_{1, 95} = 0.56$, $p > 0.05$) and the Mozambique Channel ($F_{1, 28} = 1.21$, $p > 0.05$) (Fig.
315 6).

316

317 **4. Discussion**

318 To our knowledge, this study is the first to investigate Hg concentrations in pelagic nekton
319 assemblages in the south-western Indian Ocean, including two yet undocumented shallow
320 seamounts. While Hg concentrations were relatively homogeneous in micronekton sampled
321 at the seamounts, the open ocean and the Mascarene shelf, other factors such as vertical
322 distribution, body size and trophic position may influence Hg levels.

323 4.1 Spatial variability in Hg concentrations in the south-western Indian Ocean

324 Average Hg concentrations in organisms collected at Reunion Island were lower compared to
325 those from the southern Mozambique Channel and at La Pérouse and MAD-Ridge
326 seamounts. However, no significant differences were found in Hg concentrations of the most

327 common and similar taxa between the four sampling sites. Although higher levels of methyl
328 mercury (MeHg) have been recorded in areas of higher productivity due to relatively active
329 microbial activity (Topping and Davies, 1981; Ferriss and Essington, 2014; Laurier et al.,
330 2004; Zhang et al., 2020), levels of Hg in micronekton sampled at the more productive MAD-
331 Ridge seamount and the southern Mozambique Channel were not significantly different from
332 those collected at the oligotrophic La Pérouse seamount. The lack of difference in Hg
333 between the study sites is possibly due to horizontal migratory behaviour of micronekton.
334 MeHg concentrations in micronekton may also be likely influenced by its concentrations in
335 zooplanktonic prey, with concentrations of MeHg in zooplankton being influenced by the
336 concentrations found in various phytoplankton species (Zhang et al., 2020). Future work is
337 necessary to determine Hg speciation in zooplankton so as to investigate the trophic transfer
338 of Hg between zooplankton and micronekton.

339 The Hg concentrations in mesopelagic fishes from the four study sites in the Indian Ocean
340 were higher ($0.08\text{-}1.4\ \mu\text{g g}^{-1}\ \text{dw}$) than concentrations recorded for similar specimens with
341 similar or higher size ranges (*Cyclothone* sp., *C. warmingii*, *Chauliodus sloani*, *Sigmops*
342 *elongatus*, and *Idiacanthus fasciola*) collected from the Sulu, Celebes and Philippine Seas
343 ($0.05\ \mu\text{g g}^{-1}\ \text{dw}$) (Asante et al., 2010). The crustaceans Oplophoridae and Sergestidae also
344 showed higher Hg concentrations of $0.00\text{-}1.69$ and $0.06\text{-}0.38\ \mu\text{g g}^{-1}\ \text{dw}$, respectively, relative
345 to smaller individuals collected off Niolam Island within the Papua New Guinea Province
346 where values ranged from $\sim 0.1\text{-}0.2\ \mu\text{g g}^{-1}\ \text{dw}$ for Oplophoridae and less than $0.1\ \mu\text{g g}^{-1}\ \text{dw}$
347 for Sergestidae (Brewer et al., 2012). These spatial differences operating at large ocean scale
348 could potentially reflect variations in the local net production and bioavailability of MeHg at
349 the base of the foodweb (Chakraborty et al., 2016) and/or differences in the vertical niche
350 occupied by these organisms that may also vary among ocean regions. Further research is

351 needed to provide precise MeHg depth water profiles to further address the questions behind
352 these spatial differences.

353 4.2 Vertical distribution of Hg concentrations

354 Hg concentrations in the sampled micronekton increased from organisms collected near the
355 surface (Epipelagic-Mesopelagic) to deeper parts (Mesobenthopelagic). MeHg has long been
356 thought to originate from marine sediments leading to the bioaccumulation of Hg in soft
357 tissues of organisms (Fitzgerald et al., 2007; Chakraborty and Babu, 2015; Chakraborty et al.,
358 2016; Chakraborty et al., 2019; Padalkar et al., 2019; Chennuri et al., 2020) from lower to
359 higher trophic compartments. Recent mass balance estimates suggest that the stock of marine
360 MeHg cannot be solely supplied by shelf/margin or deep sediment source (Mason et al.,
361 2012). MeHg depth profiles in the open ocean consistently show MeHg production and
362 accumulation in the subthermocline oxygen minimum zone (Cossa et al., 2009; Heimbürger
363 et al., 2010). Sulfate-reducing bacteria (Compeau and Bartha, 1985; Benoit et al., 2001;
364 Ranchou-Peyruse et al., 2009), and other anaerobic microorganisms involved in the
365 remineralization of organic matter and hosting specific methylation genes have been
366 identified as possible methylators at ocean depth (Gilmour et al., 2013; Parks et al. 2013).
367 The nine *Onychoteuthis* sp. squid specimens showing epipelagic-mesopelagic habitat ranges
368 were collected within the first 250 m of the water column from Reunion Island, and showed
369 Hg concentrations in the range of 0.02-0.08 $\mu\text{g g}^{-1}$ dw. All other organisms from Reunion
370 Island were also collected in the first 250 m but they showed mesopelagic and bathypelagic
371 habitat ranges unlike *Onychoteuthis* sp., i.e. they migrate vertically and reside deeper in the
372 water column during the day, potentially having access to a wider range of prey from
373 different habitat ranges and having higher Hg burdens.

374 The five organisms classified as benthopelagic were all fishes collected from MAD-Ridge
375 seamount (two flank-associated *N. macrolepidotus*, one flank-associated *Neoscopelus*
376 *microchir* and two summit-associated *Cookeolus japonicus*) which showed concentrations of
377 0.20-0.64 $\mu\text{g g}^{-1}$ dw. These species showed high trophic levels of 4 and were all seamount-
378 associated, hence being close to the MAD-Ridge seamount sediments, thus possibly
379 accounting for their higher Hg concentrations compared to epipelagic species. Enhanced Hg
380 bioaccumulation was found in mesopelagic prey species compared to epipelagic ones in
381 several ecosystems (Monteiro et al., 1996; Choy et al., 2009; Choy, 2013; Chouvelon et al.,
382 2012). Authors have reported a four-fold increase in Hg concentrations from epipelagic to
383 mesopelagic species (Monteiro et al., 1996), with seabirds feeding on mesopelagic prey also
384 exhibiting a four-fold increase in Hg levels in breast feathers compared to those feeding on
385 epipelagic prey (Monteiro et al., 1998). The data collected during this study suggest
386 approximately a three-fold increase in mean Hg concentrations from epipelagic to
387 mesopelagic species.

388 4.3 Factors influencing Hg concentrations in micronekton

389 Body size of organisms in the Mozambique Channel and at Reunion Island and trophic
390 position at MAD-Ridge seamount and the Mozambique Channel were shown to significantly
391 influence Hg concentrations in micronekton. Different marine organisms absorb Hg *via*
392 different pathways, either through adsorption on to the cell membrane and diffusion into
393 cells, or through suspended particles and sediments, through the gills, or from their prey
394 (Bryan et al., 1979). The individuals sampled at the different study sites may show
395 differences in Hg accumulation possibly due to differential uptake and elimination, different
396 trophic relationships, behaviours and habitat uses. Mercury concentrations typically show a
397 positive relationship with fish age and increasing size (Cai et al., 2007; Choy et al., 2009;
398 Hanchet et al., 2012; Boalt et al., 2014; Chen et al., 2014) as a result of longer exposure time

399 to the trace element (Pellegrini and Barghigiani, 1989), intake rates exceeding excretion rates
400 (Cai et al., 2007; Houssard et al., 2019) and/or a shift in diet (Mason et al., 2000), with larger
401 fishes attaining higher body sizes and feeding at higher trophic levels (Cai et al., 2007).
402 Larger zooplankton types have higher MeHg concentrations than smaller species (Zhang et
403 al., 2020). Micronekton species feeding on larger zooplankton, would thus possibly show
404 higher MeHg concentrations relative to those feeding on smaller zooplankton.

405 Compared to studies which showed Hg concentrations lower than the detection limit (<0.05
406 $\mu\text{g g}^{-1}$ dw) in small-sized mesopelagic fishes sampled in the Sulu and Celebes Seas in the
407 south-western area of the Philippines, only nine among 174 fishes sampled at the four study
408 sites in the Indian Ocean showed Hg concentrations $<0.05 \mu\text{g g}^{-1}$ dw and $\delta^{15}\text{N}$ and TL values
409 from 6.0 to 10.2‰ and 2.6 to 3.9, respectively. In fact, seven carnivorous fishes (five from
410 MAD-Ridge, one from the Mozambique Channel and one from Reunion Island) showed Hg
411 concentrations $>0.5 \mu\text{g g}^{-1}$ dw. These fish include two mesopelagic *A. aculeatus* (54.4 and
412 77.3 mm), one bathypelagic *Neoscopelus macrolepidotus* (46 mm), one seamount-associated
413 *Diaphus suborbitalis* (81.2 mm), one mesopelagic *Astronesthes* (122.3 mm), one
414 bathypelagic *Stomias longibarbatus* (371 mm) and one mesopelagic *Sigmops elongatus*
415 (173.8 mm). The $\delta^{15}\text{N}$ of these fishes ranged from 9.2 to 11.8‰, i.e. from TL 3.6 to 4.4. All
416 other fishes showed Hg concentrations $<0.5 \mu\text{g g}^{-1}$ dw, despite some of them being
417 bathypelagic, having high body sizes and $\delta^{15}\text{N}$ values. In addition to habitat range, size and
418 trophic level, some other factors may hence influence Hg concentration in mesopelagic
419 fishes. Small fish such as *A. aculeatus* previously reported as residents of deep-water layers
420 in the Pacific (Receveur et al., 2020) and sampled in greater proportions below 400 m during
421 both day and night at MAD-Ridge seamount (Annasawmy et al., 2019) may show high Hg
422 concentrations because of their deep habitat range and absence of diel vertical migration.
423 Differences in trace element concentrations were also found between migrant and non-

424 migrant deep-water mesopelagic fish in the south-western Philippines (Asante et al., 2010).
425 The skin of *A. aculeatus*, which is difficult to dissociate from the tissue during the sampling
426 process, may also be an important site for metal uptake due to their high surface area to body
427 ratio as shown for other fish species (Afandi et al., 2018), thus contributing to higher overall
428 Hg concentrations.

429 The two *O. bartramii* specimens sampled at MAD-Ridge and the southern Mozambique
430 Channel were the only squids showing Hg concentrations greater than 0.5 $\mu\text{g g}^{-1}$ dw. Squids
431 also showed higher Hg concentrations relative to the fish species Acanthuridae,
432 Monacanthidae and *Stolephorus* sp. off Niolam Island within the Papua New Guinea
433 Province (Brewer et al., 2012). The *O. bartramii* had higher TL of 4.8 and 5.0 than the other
434 sampled micronekton taxa and are known to feed on mesopelagic fish and other cephalopods
435 (Hastie et al., 2009; Coll et al., 2013; Navarro et al., 2013), thus bioaccumulating Hg
436 concentrations from their micronektonic prey. Size and hence age might be a factor
437 influencing Hg concentrations in the *O. bartramii* specimens which had DML of 365 and 490
438 mm relative to the other smaller sampled squids which ranged in size from 18 mm
439 (*Abraliopsis* sp.) to 163 mm (*Ornithoteuthis volatilis*). Shorter life span of some species may
440 further reduce their exposure to Hg (Pellegrini and Barghigiani, 1989) relative to species
441 having longer life spans and hence potentially showing higher Hg concentrations due to
442 persistent exposure over time.

443 4.4 Biomagnification of Hg in pelagic nekton assemblages

444 Biomagnification of Hg along marine food webs has been previously investigated using
445 stable isotope analyses (Asante et al., 2008). Previous studies have shown positive
446 relationships between $\delta^{13}\text{C}$ and $\delta^{15}\text{N}$ values and concentrations of trace elements in
447 micronekton, suggesting biomagnification of these chemicals (Asante et al., 2008, 2010). The

448 lack of clear relationship between Hg concentrations and $\delta^{13}\text{C}$ values may be attributed to
449 micronekton across the four sites having offshore/pelagic habitats with no
450 inshore/coastal/demersal inputs (Goutte et al., 2015; Le Croizier et al., 2019). The positive
451 relationships between Hg levels and stable nitrogen isotope values in micronekton collected
452 at MAD-Ridge seamount and the southern Mozambique Channel, suggests biomagnification
453 of Hg through the food webs that characterise these ecosystems. This might imply that higher
454 trophic mesopelagic organisms retained higher Hg concentrations than lower trophic ones
455 (Asante et al., 2008). Increases in Hg concentrations with trophic position were observed
456 across zooplankton, micronekton and large predators in the North Pacific subtropical gyre
457 (Choy, 2013). Significant positive relationships between Hg concentration and trophic
458 position were also observed in pelagic marine top predators (Storelli et al., 2005; Cai et al.,
459 2007; Bodin et al., 2017) due to organisms feeding at higher trophic positions consuming
460 larger prey with higher body burdens than smaller prey (Watras et al., 1998; Bowles et al.,
461 2001; Cai et al., 2007). The lack of relationship between Hg and $\delta^{15}\text{N}$ values at La Pérouse
462 may be attributed to the complex food webs in oligotrophic tropical ecosystems with variable
463 Hg concentrations as observed in previous tropical ecosystems (Al-Reasi et al., 2007).

464 The length of the studied food chains at La Pérouse, MAD-Ridge and the Mozambique
465 Channel may also explain the difference in Hg biomagnification observed in micronekton
466 between sites. While a two-step (3 trophic levels) pelagic food chain has been observed at La
467 Pérouse, a three-step (4 trophic levels) food chain has been observed at MAD-Ridge and in
468 the Mozambique Channel due to the sampling of micronekton feeding *O. bartramii*
469 specimens at the two later sites (Annasawmy et al., 2020b). Higher trophic level organisms
470 such as large squids which potentially have high Hg concentrations and possibly account for
471 Hg biomagnification were not sampled during La Pérouse cruise possibly due to their net
472 avoidance abilities and smaller number of trawls conducted relative to MAD-Ridge cruise.

473 Previous studies have found differences in the degree of trace metal biomagnification
474 between Clearwater Bay and Butterfly Bay from Hong Kong because of the length of the
475 food webs at these two sites (Cheung and Wang, 2008). Similar to our results, other studies
476 on albacore, yellowfin and bigeye tunas in the western and central Pacific have found that
477 trophic effects on Hg concentrations are of lower importance relative to foraging depth and
478 feeding ecology (Houssard et al., 2019).

479 **Limits and perspectives**

480 Since research was conducted during a declining phase of productivity in the region
481 (Annasawmy et al., 2019) the full variability in stable isotope and Hg concentrations may not
482 have been captured. This work is the first to investigate Hg concentrations in pelagic nekton
483 organisms at only four sites in the Indian Ocean (two shallow seamounts, the Mascarene shelf
484 and the open ocean). Further studies will be conducted to investigate trace mineral
485 concentrations in pelagic nekton at other sites influenced by riverine input such as the African
486 shelf in the Mozambique Channel and open areas in the north-western and southern Indian
487 Ocean. Additional insights could have been gained with the investigation of Hg
488 concentrations in the water column and the relationship between sedimentary organic matter
489 and Hg of the south-western Indian Ocean. Organisms may also incorporate the isotopic
490 signal and Hg concentrations of their diets at varying rates and within varying tissues in their
491 body (Martínez del Rio et al., 2009; Afandi et al., 2018). The incomplete inclusion of the
492 entire food web at La Pérouse may result in the absence of biomagnification of Hg observed
493 at the seamount. The full variability in Hg concentrations within pelagic nekton assemblages
494 could not be further described due to limited information on Hg concentrations within lower
495 trophic compartments. Future work will investigate the Hg concentrations within various
496 tissues in similar organisms and in lower trophic compartments.

498 **Acknowledgements**

499 The authors acknowledge the work carried by the non-scientific staff on board the R/V
500 ANTEA and the scientific staff onboard and on land, including Yves Cherel (CNRS, La
501 Rochelle, France), Delphine Thibault (MIO, Marseille, France) and P. Alexander Hulley
502 (South Africa) for identifying the micronekton taxa, and Hervé Demarcq (IRD, Sète, France)
503 for providing the SSC data. The authors also acknowledge the assistance and support of the
504 chief scientists Francis Marsac for La Pérouse, Jean-François Ternon for MAD-Ridge cruises
505 (IRD, Sète, France) and Sebastien Jaquemet (Université de la Réunion) for IOTA cruise, and
506 the Master BEST-ALI students who helped with the collection of samples. The authors
507 further appreciate the assistance of Gaël Le Croizier for the mercury analyses conducted at
508 the GET (Toulouse, France) and François Le Loc'h for the stable isotope analyses at the Pôle
509 de Spectrométrie Océan (Plouzané, France). The data collection was mainly supported by the
510 Flotte Oceanographique Française (French Oceanographic Fleet) and IRD in relation to the
511 logistics of the R/V ANTEA. Additional funding was received from the Conseil Régional de
512 la Reunion (Reunion Regional Council, Bop 123/2016) for La Pérouse cruise, and from the
513 Fonds Français pour l'Environnement Mondial (FFEM) as part of the FFEM-SWIO project
514 on Areas Beyond National Jurisdiction (ABNJ) of the South West Indian Ocean for MAD-
515 Ridge cruise. This work was financially supported by the French National Research Agency
516 project ANR-17-CE34-0010 MERTOX (PI David Point). Pavanee Annasawmy is the
517 beneficiary of a MARG-I bursary granted by the WIOMSA (Western Indian Ocean Marine
518 Science Association) and the EuroMarine Network's (<http://www.euromarinenetwork.eu/>)
519 Individual Fellowship Programme 2019. The Seychelles Fishing Authority is acknowledged
520 for help with coordinating the WIOMSA MARG-I funding.

521

522 **References**

- 523 Afandi, I., Talba, S., Benhra, A., Benbrahim, S., Chfiri, R., Labonne, M., Masski, H., Laë, R.,
524 Tito De Morais, L., Bekkali, M., Bouthir, F.Z., 2018. Trace metal distribution in
525 pelagic fish species from the north-west African coast (Morocco). *International*
526 *Aquatic Research* 10, 191–205. <https://doi.org/10.1007/s40071-018-0192-7>
- 527 Al-Reasi, H.A., Ababneh, F.A., Lean, D.R., 2007. Evaluating mercury biomagnification in
528 fish from a tropical marine environment using stable isotopes ($\delta^{13}\text{C}$ and $\delta^{15}\text{N}$).
529 *Environmental Toxicology and Chemistry* 26, 1572. [https://doi.org/10.1897/06-](https://doi.org/10.1897/06-359R.1)
530 359R.1

531 Alverson, F.G., 1961. Daylight Surface Occurrence of Myctophid Fishes off the coast of
532 Central America. *Pacific Science*, 15(3), 35-43.

533 Annasawmy, P., Ternon, J-F., Lebourges-Dhaussy, A., Roudaut, G., Herbette, S., Ménard, F.,
534 Cotel, P., Marsac, F., 2020a. Micronekton distribution as influenced by mesoscale
535 eddies, Madagascar shelf and shallow seamounts in the south-western Indian Ocean:
536 an acoustic approach. *Deep-Sea Res. II*. <https://doi.org/10.1016/j.dsr2.2020.104812>

537 Annasawmy, P., Cherel, Y., Romanov, E.V., Le Loch, F., Ménard, F., Ternon, J-F., Marsac,
538 F., 2020b. Stable isotope patterns of micronekton at two shallow seamounts of the
539 south-western Indian Ocean. *Deep-Sea Res. II*.
540 <https://doi.org/10.1016/j.dsr2.2020.104804>

541 Annasawmy, P., Ternon, J.-F., Cotel, P., Cherel, Y., Romanov, E.V., Roudaut, G.,
542 Lebourges-Dhaussy, A., Ménard, F., Marsac, F., 2019. Micronekton distributions and
543 assemblages at two shallow seamounts of the south-western Indian Ocean: Insights
544 from acoustics and mesopelagic trawl data. *Progress in Oceanography* 178, 102161.
545 <https://doi.org/10.1016/j.pocean.2019.102161>

546 Annasawmy, P., Ternon, J.F., Marsac, F., Cherel, Y., Béhagle, N., Roudaut, G., Lebourges-
547 Dhaussy, A., Demarcq, H., Moloney, C.L., Jaquemet, S., Ménard, F., 2018.
548 Micronekton diel migration, community composition and trophic position within two
549 biogeochemical provinces of the South West Indian Ocean: Insight from acoustics
550 and stable isotopes. *Deep Sea Research Part I: Oceanographic Research Papers* 138,
551 85–97. <https://doi.org/10.1016/j.dsr.2018.07.002>

552 Ariza, V. A., 2015. Micronekton diel vertical migration and active flux in the subtropical
553 Northeast Atlantic. Universidad de Las Palmas de Gran Canaria. Doctoral Thesis.

554 Ariza, A., Garijo, J.C., Landeira, J.M., Bordes, F., Hernández-León, S., 2015. Migrant
555 biomass and respiratory carbon flux by zooplankton and micronekton in the
556 subtropical northeast Atlantic Ocean (Canary Islands). *Progress in Oceanography* 134,
557 330–342. <https://doi.org/10.1016/j.pocean.2015.03.003>

558 Asante, K.A., Agusa, T., Kubota, R., Mochizuki, H., Ramu, K., Nishida, S., Ohta, S., Yeh,
559 H., Subramanian, A., Tanabe, S., 2010. Trace elements and stable isotope ratios ($\delta^{13}\text{C}$
560 and $\delta^{15}\text{N}$) in fish from deep-waters of the Sulu Sea and the Celebes Sea. *Marine*
561 *Pollution Bulletin* 60, 1560–1570. <https://doi.org/10.1016/j.marpolbul.2010.04.011>

562 Asante, K.A., Agusa, T., Mochizuki, H., Ramu, K., Inoue, S., Kubodera, T., Takahashi, S.,
563 Subramanian, A., Tanabe, S., 2008. Trace elements and stable isotopes ($\delta^{13}\text{C}$ and
564 $\delta^{15}\text{N}$) in shallow and deep-water organisms from the East China Sea. *Environmental*
565 *Pollution* 156, 862–873. <https://doi.org/10.1016/j.envpol.2008.05.020>

566 Atkinson, A., Siegel, V., Pakhomov, E.A., Jessopp, M.J., Loeb, V., 2009. A re-appraisal of
567 the total biomass and annual production of Antarctic krill. *Deep Sea Research Part I:*
568 *Oceanographic Research Papers* 56, 727–740.
569 <https://doi.org/10.1016/j.dsr.2008.12.007>

570 Bartlett, M.S., 1937. Properties of sufficiency and statistical tests. *Proc. R. Soc. Lond. A* 160,
571 268–282. <https://doi.org/10.1098/rspa.1937.0109>.

572 Béhagle, N., du Buisson, L., Josse, E., Lebourges-Dhaussy, A., Roudaut, G., Ménard, F.,
573 2014. Mesoscale features and micronekton in the Mozambique Channel: An acoustic
574 approach. *Deep Sea Research Part II: Topical Studies in Oceanography* 100, 164–173.
575 <https://doi.org/10.1016/j.dsr2.2013.10.024>

576 Benoit, J.M., Gilmour, C.C., Mason, R.P., 2001. Aspects of bioavailability of mercury for
577 methylation cultures of *Desulfobulbus propionicus* (1pr3). *Applied and Environmental*
578 *Microbiology* 67(1): 51-58. 10.1128/AEM.67.1.51–58.2001

- 579 Bernal, A., Olivar, M.P., Maynou, F., Fernández de Puellas, M.L., 2015. Diet and feeding
580 strategies of mesopelagic fishes in the western Mediterranean. *Progress in*
581 *Oceanography* 135, 1–17. <https://doi.org/10.1016/j.pocean.2015.03.005>
- 582 Birkley, S.-R., Gulliksen, B., 2003. Feeding Ecology in Five Shrimp Species (Decapoda,
583 Caridea) from an Arctic Fjord (Isfjorden, Svalbard), with Emphasis on *Sclerocrangon*
584 *boreas*. Phipps.
- 585 Bloom, N.S., 1992. On the Chemical Form of Mercury in Edible Fish and Marine
586 Invertebrate Tissue. *Canadian Journal of Fisheries and Aquatic Sciences* 49, 1010–
587 1017. <https://doi.org/10.1139/f92-113>
- 588 Blum, J.D., Popp, B.N., Drazen, J.C., Anela Choy, C., Johnson, M.W., 2013. Methylmercury
589 production below the mixed layer in the North Pacific Ocean. *Nature Geoscience* 6,
590 879–884. <https://doi.org/10.1038/ngeo1918>
- 591 Boalt, E., Miller, A., Dahlgren, H., 2014. Distribution of cadmium, mercury, and lead in
592 different body parts of Baltic herring (*Clupea harengus*) and perch (*Perca fluviatilis*):
593 Implications for environmental status assessments. *Marine Pollution Bulletin* 78, 130–
594 136. <https://doi.org/10.1016/j.marpolbul.2013.10.051>
- 595 Bodin, N., Lesperance, D., Albert, R., Hollanda, S., Michaud, P., Degroote, M., Churlaud, C.,
596 Bustamante, P., 2017. Trace elements in oceanic pelagic communities in the western
597 Indian Ocean. *Chemosphere* 174, 354–362.
598 <https://doi.org/10.1016/j.chemosphere.2017.01.099>
- 599 Bodin, N., Budzinski, H., Le Ménach, K., Tapie, N., 2009. ASE extraction method for
600 simultaneous carbon and nitrogen stable isotope analysis in soft tissues of aquatic
601 organisms. *Analytica Chimica Acta* 643, 54–60.
602 <https://doi.org/10.1016/j.aca.2009.03.048>
- 603 Bowles, K. C., Apte, S. C., Maher, W. A., Kawei, M., Smith, R., 2001. Bioaccumulation and
604 biomagnification of mercury in lake Murray, Papua New Guinea. *Canadian Journal of*
605 *Fisheries and Aquatic Sciences*, 58(5), 888-897.
- 606 Brewer, D.T., Morello, E.B., Griffiths, S., Fry, G., Heales, D., Apte, S.C., Venables, W.N.,
607 Rothlisberg, P.C., Moeseneder, C., Lansdell, M., Pendrey, R., Coman, F., Strzelecki,
608 J., Jarolimek, C.V., Jung, R.F., Richardson, A.J., 2012. Impacts of gold mine waste
609 disposal on a tropical pelagic ecosystem. *Marine Pollution Bulletin* 64, 2790–2806.
610 <https://doi.org/10.1016/j.marpolbul.2012.09.009>
- 611 Briand, M.J., Bustamante, P., Bonnet, X., Churlaud, C., Letourneur, Y., 2018. Tracking trace
612 elements into complex coral reef trophic networks. *Science of The Total Environment*
613 612, 1091–1104. <https://doi.org/10.1016/j.scitotenv.2017.08.257>
- 614 Brodeur, R., Yamamura, O., 2005. PICES Scientific Report No. 30 Micronekton of the North
615 Pacific. PICES Scientific Report, Sidney, B.C., Canada, pp. 1–115.
- 616 Bryan, G. W., Waldichuk, M., Pentreath, R.J., Darracott, A., 1979. Bioaccumulation of
617 marine pollutants. *Philosophical Transactions of the Royal Society of London. B,*
618 *Biological Sciences*, 286(1015), 483-505.
- 619 Bustamante, P., Lahaye, V., Durnez, C., Churlaud, C., Caurant, F., 2006. Total and organic
620 Hg concentrations in cephalopods from the North Eastern Atlantic waters: Influence
621 of geographical origin and feeding ecology. *Science of The Total Environment* 368,
622 585–596. <https://doi.org/10.1016/j.scitotenv.2006.01.038>
- 623 Cai, Y., Rooker, J.R., Gill, G.A., Turner, J.P., 2007. Bioaccumulation of mercury in pelagic
624 fishes from the northern Gulf of Mexico. *Canadian Journal of Fisheries and Aquatic*
625 *Sciences* 64, 458–469. <https://doi.org/10.1139/f07-017>
- 626 Calatayud, M., Devesa, V., Virseda, J.R., Barberá, R., Montoro, R., Vélez, D., 2012. Mercury
627 and selenium in fish and shellfish: Occurrence, bioaccessibility and uptake by Caco-2

628 cells. Food and Chemical Toxicology 50, 2696–2702.
629 <https://doi.org/10.1016/j.fct.2012.05.028>

630 Carmo, V., Sutton, T., Menezes, G., Falkenhaus, T., Bergstad, O.A., 2015. Feeding ecology
631 of the Stomiiformes (Pisces) of the northern Mid-Atlantic Ridge. 1. The
632 Sternoptychidae and Phosichthyidae. Progress in Oceanography 130, 172–187.
633 <https://doi.org/10.1016/j.pocean.2014.11.003>

634 Chai, H.-J., Chan, Y.-L., Li, T.-L., Chen, Y.-C., Wu, C.-H., Shiau, C.-Y., Wu, C.-J., 2012.
635 Composition characterization of Myctophids (*Benthosema pterotum*): Antioxidation
636 and safety evaluations for Myctophids protein hydrolysates. Food Research
637 International 46, 118–126. <https://doi.org/10.1016/j.foodres.2011.12.008>

638 Chakraborty, P., Babu, P.V.R., 2015. Environmental controls on the speciation and
639 distribution of mercury in surface sediments of a tropical estuary, India. Marine
640 Pollution Bulletin 95, 350–357. <http://dx.doi.org/10.1016/j.marpolbul.2015.02.035>

641 Chakraborty, P., Mason, R.P., Jayachandran, S., Vudamala, K., Armoury, K., Sarkar, A.,
642 Chakraborty, S., Bardhan, P., Naik, R., 2016. Effects of bottom water oxygen
643 concentrations on mercury distribution and speciation in sediments below the oxygen
644 minimum zone of the Arabian Sea. Marine Chemistry 186, 24–32.
645 <http://dx.doi.org/10.1016/j.marchem.2016.07.005>

646 Chakraborty, P., Jayachandran, S., Lekshmy, J., Padalkar, P., Sitlhou, L., Chennuri, K.,
647 Shetye, S., Sardar, A., Khandeparker, R., 2019. Seawater intrusion and resuspension
648 of surface sediment control mercury (Hg) distribution and its bioavailability in water
649 column of a monsoonal estuarine system. Science of the Total Environment 660,
650 1441–1448. <https://doi.org/10.1016/j.scitotenv.2018.12.477>

651 Chen, C.-Y., Lai, C.-C., Chen, K.-S., Hsu, C.-C., Hung, C.-C., Chen, M.-H., 2014. Total and
652 organic mercury concentrations in the muscles of Pacific albacore (*Thunnus alalunga*)
653 and bigeye tuna (*Thunnus obesus*). Marine Pollution Bulletin 85, 606–612.
654 <https://doi.org/10.1016/j.marpolbul.2014.01.039>

655 Chennuri, K., Chakraborty, P., Jayachandran, S., Mohakud, S.K., Ishita, I., Ramteke, D.,
656 Padalkar, P.P., Babu, P.C., Babu, K.R., 2020. Operationally defined mercury (Hg)
657 species can delineate Hg bioaccumulation in mangrove sediment systems: A case
658 study. Science of the Total Environment 701, 134842.
659 <https://doi.org/10.1016/j.scitotenv.2019.134842>

660 Cheung, M.S., Wang, W.-X., 2008. Analyzing biomagnification of metals in different marine
661 food webs using nitrogen isotopes. Marine Pollution Bulletin 56, 2082–2088.
662 <https://doi.org/10.1016/j.marpolbul.2008.09.004>

663 Chauvelon, T., Brach-Papa, C., Auger, D., Bodin, N., Bruzac, S., Crochet, S., Degroote, M.,
664 Hollanda, S.J., Hubert, C., Knoery, J., Munsch, C., Puech, A., Rozuel, E., Thomas,
665 B., West, W., Bourjea, J., Nikolic, N., 2017. Chemical contaminants (trace metals,
666 persistent organic pollutants) in albacore tuna from western Indian and south-eastern
667 Atlantic Oceans: Trophic influence and potential as tracers of populations. Science of
668 The Total Environment 596–597, 481–495.
669 <https://doi.org/10.1016/j.scitotenv.2017.04.048>

670 Chauvelon, T., Spitz, J., Caurant, F., Mèndez-Fernandez, P., Autier, J., Lassus-Débat, A.,
671 Chappuis, A., Bustamante, P., 2012. Enhanced bioaccumulation of mercury in deep-
672 sea fauna from the Bay of Biscay (north-east Atlantic) in relation to trophic positions
673 identified by analysis of carbon and nitrogen stable isotopes. Deep Sea Research Part
674 I: Oceanographic Research Papers, 65, 113–124.

675 Choy, C., 2013. Pelagic food web connectivity in the North Pacific Subtropical Gyre: a
676 combined perspective from multiple biochemical tracers and diet. University of
677 Hawaii, Manoa. Doctoral Thesis.

- 678 Choy, C.A., Popp, B.N., Kaneko, J.J., Drazen, J.C., 2009. The influence of depth on mercury
679 levels in pelagic fishes and their prey. *Proceedings of the National Academy of*
680 *Sciences* 106, 13865–13869. <https://doi.org/10.1073/pnas.0900711106>
- 681 Clarke, M.R., Lu, C.C., 1975. Vertical distribution of cephalopods at 18°N 25°W in the North
682 Atlantic. *Journal of the Marine Biological Association of the United Kingdom* 55,
683 165. <https://doi.org/10.1017/S0025315400015812>
- 684 Coll, M., Navarro, J., Olson, R.J., Christensen, V., 2013. Assessing the trophic position and
685 ecological role of squids in marine ecosystems by means of food-web models. *Deep*
686 *Sea Research Part II: Topical Studies in Oceanography* 95, 21–36.
687 <https://doi.org/10.1016/j.dsr2.2012.08.020>
- 688 Compeau, G.C., Bartha, R., 1985. Sulfate-Reducing Bacteria: Principal Methylators of
689 Mercury in Anoxic Estuarine Sediment. *Applied and Environmental Microbiology*
690 50(2), 498-502.
- 691 Cossa, D., Thibaud, Y., Roméo, M., Gnassia-Barelli, M., 1990. Le mercure en milieu marin.
692 *Biogéochimie et Ecotoxicologie. Rapports scientifiques et techniques de l'IFREMER,*
693 N° 19.
- 694 Cossa, D., Averty, B., Pirrone, N., 2009. The origin of methylmercury in open Mediterranean
695 waters. *Limnology and Oceanography* 54, 837–844.
696 <https://doi.org/10.4319/lo.2009.54.3.0837>
- 697 Dalpadado, P., Gjørseter, J., 1988. Feeding ecology of the lanternfish *Benthosema pterotum*
698 from the Indian Ocean. *Mar. Biol.* 99, 555–567.
- 699 Davison, P.C., Koslow, J.A., Kloser, R.J., 2015. Acoustic biomass estimation of mesopelagic
700 fish: backscattering from individuals, populations, and communities. *ICES Jour.*
701 *Mar.Sci.* 72 (5), 1413–1424. <https://doi.org/10.1093/icesjms/fsv023>.
- 702 De Forest, L., Drazen, J., 2009. The influence of a Hawaiian seamount on mesopelagic
703 micronekton. *Deep Sea Research Part I: Oceanographic Research Papers* 56, 232–
704 250. <https://doi.org/10.1016/j.dsr.2008.09.007>
- 705 Del Giorgio, P.A., Duarte, C.M., 2002. Respiration in the open ocean. *Nature* 420, 379–384.
- 706 Ferriss, B. E., Essington, T. E., 2014. Does trophic structure dictate mercury concentrations
707 in top predators? A comparative analysis of pelagic food webs in the Pacific Ocean.
708 *Ecological modelling*, 278, 18-28.
- 709 Filmlalter, J. D., Cowley, P. D., Potier, M., Ménard, F., Smale, M. J., Cherel, Y., Dagorn, L.,
710 2017. Feeding ecology of silky sharks *Carcharhinus falciformis* associated with
711 floating objects in the western Indian Ocean. *Journal of Fish Biology*, 90, 1321–1337.
712 <https://doi.org/10.1111/jfb.13241>
- 713 Fitzgerald, W. F., Lamborg, C. H., Hammerschmidt, C. R., 2007. Marine biogeochemical
714 cycling of mercury. *Chemical Reviews*, 107(2), 641–662.
715 <https://doi.org/10.1021/cr050353m>
- 716 Foxton, P., Roe, H.S.J., 1974. Observations on the nocturnal feeding of some mesopelagic
717 decapod Crustacea. *Mar. Biol.* 28, 37–49.
- 718 Gilmour, C.C., Podar, M., Bullock, A.L., Graham, A.M., Brown, S.D., Somenahally, A.C.,
719 Johs, A., Hurt, Jr., R.A., Bailey, K.L., Elias, D.A., 2013. Mercury Methylation by
720 Novel Microorganisms from New Environments. *Environmental Science &*
721 *Technology* 47, 11810-11820.
- 722 Goutte, A., Cherel, Y., Churlaud, C., Ponthus, J-P., Massé, G., Bustamante, P., 2015. Trace
723 elements in Antarctic fish species and the influence of foraging habitats and dietary
724 habits on mercury levels. *Science of the Total Environment* 538, 743-749.
725 <http://dx.doi.org/10.1016/j.scitotenv.2015.08.103>
- 726 Gray, J.S., 2002. Biomagnification in marine systems: the perspective of an ecologist. *Marine*
727 *Pollution Bulletin* 45, 46–52. [https://doi.org/10.1016/S0025-326X\(01\)00323-X](https://doi.org/10.1016/S0025-326X(01)00323-X)

- 728 Gjørseter, J. 1984. Mesopelagic fish, a large potential resource in the Arabian Sea. Deep Sea
729 Research Part A. Oceanographic Research Papers, 31(6-8), 1019-1035.
- 730 Gjørseter, J. 1977. Aspects of the distribution and ecology of the Myctophidae from the
731 western and northern Arabian Sea. Department of Fisheries Biology, University of
732 Bergen.
- 733 Guinet, C., Cherel, Y., Ridoux, V., Jouventin, P., 1996. Consumption of marine resources by
734 seabirds and seals in Crozet and Kerguelen waters: changes in relation to consumer
735 biomass 1962–85. Antarctic Science 8. <https://doi.org/10.1017/S0954102096000053>
- 736 Hanchet, S.M., Tracey, D., Dunn, A., Horn, P., Smith, N., 2012. Mercury concentrations of
737 two toothfish and three of its prey species from the Pacific sector of the Antarctic.
738 Antarctic Science 24, 34–42. <https://doi.org/10.1017/S0954102011000654>
- 739 Hastie, L. C., Pierce, G. J., Wang, J., Bruno, I., Moreno, A., Piatkowski, U., Robin, J. P.,
740 2009. Cephalopods in the north-eastern Atlantic: species, biogeography, ecology,
741 exploitation and conservation. Oceanography and marine biology, 47(80), 111-190.
- 742 Heimbürger, L-E., Cossa, D., Marty, J-C., Migon, C., Averty, B., Dufour, A., Ras, J., 2010.
743 Methyl mercury distributions in relation to the presence of nano- and
744 picophytoplankton in an oceanic water column (Ligurian Sea, North-western
745 Mediterranean). Geochimica et Cosmochimica Acta 74(19): 5549-5559.
746 <http://dx.doi.org/10.1016/j.gca.2010.06.036>
- 747 Hidaka, K., Kawaguchi, K., Murakami, M., Takahashi, M., 2001. Downward transport of
748 organic carbon by diel migratory micronekton in the western equatorial Pacific: its
749 quantitative and qualitative importance. Deep-Sea Res. I. 48, 1923–1939.
- 750 Hobson, K.A., Piatt, J.F., Pitocchelli, J., 1994. Using stable isotopes to determine seabird
751 trophic relationships. J. Anim. Ecol. 63, 786–798.
- 752 Hopkins, T.L., Flock, M.E., Gartner Jr., J.V., Torres, J.J., 1994. Structure and trophic ecology
753 of a low latitude midwater decapod and mysid assemblage. Mar. Ecol. Prog. Ser. 109,
754 143–156.
- 755 Houssard, P., Point, D., Tremblay-Boyer, L., Allain, V., Pethybridge, H., Masbou, J., Ferriss,
756 B. E., Baya, P. A., Lagane, C., Menkes, C. E., Letourneur, Y., Lorrain, A., 2019. A
757 model of mercury distribution in tuna from the Western and Central Pacific Ocean:
758 Influence of Physiology, Ecology and Environmental factors. Environ. Sci. Technol.
759 53: 1422-1431. DOI: 10.1021/acs.est.8b06058
- 760 Hudson, J.M., Steinberg, D.K., Sutton, T.T., Graves, J.E., Latour, R.J., 2014. Myctophid
761 feeding ecology and carbon transport along the northern Mid-Atlantic Ridge. Deep
762 Sea Research Part I: Oceanographic Research Papers 93, 104–116.
763 <https://doi.org/10.1016/j.dsr.2014.07.002>
- 764 Irigoien, X., Klevjer, T.A., Røstad, A., Martinez, U., Boyra, G., Acuña, J.L., Bode, A.,
765 Echevarria, F., Gonzalez-Gordillo, J.I., Hernandez-Leon, S., Agusti, S., Aksnes, D.L.,
766 Duarte, C.M., Kaartvedt, S., 2014. Large mesopelagic fishes biomass and trophic
767 efficiency in the open ocean. Nature Communications 5.
768 <https://doi.org/10.1038/ncomms4271>
- 769 Jena, B., Sahu, S., Avinash, K., Swain, D., 2013. Observation of oligotrophic gyre variability
770 in the south Indian Ocean: Environmental forcing and biological response. Deep Sea
771 Research Part I: Oceanographic Research Papers 80, 1–10.
772 <https://doi.org/10.1016/j.dsr.2013.06.002>
- 773 Kojadinovic, J., Jackson, C. H., Cherel, Y., Jackson, G. D., Bustamante, P., 2011. Multi-
774 elemental concentrations in the tissues of the oceanic squid *Todarodes filippovae*
775 from Tasmania and the southern Indian Ocean. Ecotoxicology and Environmental
776 Safety, 74(5), 1238–1249. <https://doi.org/10.1016/j.ecoenv.2011.03.015>

777 Lambert, C., Mannocci, L., Lehodey, P., Ridoux, V., 2014. Predicting Cetacean Habitats
778 from Their Energetic Needs and the Distribution of Their Prey in Two Contrasted
779 Tropical Regions. PLoS ONE. 9: e105958.
780 <https://doi.org/10.1371/journal.pone.0105958>

781 Laurier, F. J. G., Mason, R. P., Gill, G. A., Whalin, L., 2004. Mercury distributions in the
782 North Pacific Ocean—20 years of observations. Marine Chemistry, 90(1-4), 3-19.

783 Lavoie, R., Jardine, T. D., Chumchall, M. M., Kidd, K. A., Campbell, L. M., 2013.
784 Biomagnification rate of mercury in aquatic food webs: a world-wide meta-analysis.
785 Environmental Science & Technology, 47(23), 13385–13394.

786 Le Croizier, G., Schaal, G., Point, D., Le Loc'h, F., Machu, E., Fall, M., Munaron, J.-M.,
787 Boyé, A., Walter, P., Laë, R., Tito De Morais, L., 2019. Stable isotope analyses
788 revealed the influence of foraging habitat on mercury accumulation in tropical coastal
789 marine fish. Science of The Total Environment 650, 2129–2140.
790 <https://doi.org/10.1016/j.scitotenv.2018.09.330>

791 Lebourges-Dhaussy, A., Marchal, É., Menkès, C., Champalbert, G., Biessy, B., 2000.
792 *Vinciguerria nimbaria* (micronekton), environment and tuna: their relationships in the
793 Eastern Tropical Atlantic. Oceanologica Acta 23, 515–528.
794 [https://doi.org/10.1016/S0399-1784\(00\)00137-7](https://doi.org/10.1016/S0399-1784(00)00137-7)

795 LeMoigne, F. A. C. 2019., Pathways of organic carbon downward transport by the oceanic
796 biological carbon pump. Front. Mar. Sci. 6(634): 1-8. doi: 10.3389/fmars.2019.00634

797 Longhurst, A., 1998. Ecological Geography of the Sea. Academic Press, San Diego, p. 398.

798 Marchal, E., Lebourges, A., 1996. Acoustic evidence for unusual diel behaviour of a
799 mesopelagic fish (*Vinciguerria nimbaria*) exploited by tuna. ICES Journal of Marine
800 Science, 53(2), 443-447.

801 Marsac, F., Annasawmy, P., Noyon, M., Demarcq, H., Soria, M., Rabearisoa, N., Bach, P.,
802 Cherel, Y., Grelet, J., Romanov, E., 2020. Seamount effect on circulation and
803 distribution of ocean taxa in the vicinity of La Pérouse, a shallow seamount in the
804 southwestern Indian Ocean. Deep Sea Research Part II: Topical Studies in
805 Oceanography, 176, 104806. <https://doi.org/10.1016/j.dsr2.2020.104806>

806 Martínez del Rio, C., Wolf, N., Carleton, S.A., Gannes, L.Z., 2009. Isotopic ecology ten
807 years after a call for more laboratory experiments. Biol. Rev. 84, 91–111. <https://doi.org/10.1111/j.1469-185X.2008.00064.x>.

809 Mason, R.P., Laporte, J.-M., Andres, S., 2000. Factors Controlling the Bioaccumulation of
810 Mercury, Methylmercury, Arsenic, Selenium, and Cadmium by Freshwater
811 Invertebrates and Fish. Archives of Environmental Contamination and Toxicology 38,
812 283–297. <https://doi.org/10.1007/s002449910038>

813 Mason, R.P., Choi, A.L., Fitzgerald, W.F., Hammerschmidt, C.R., Lamborg, C.H.,
814 Soerensen, A. L., Sunderland, E.M., 2012 Mercury biogeochemical cycling in the
815 ocean and policy implications. Environmental Research 119, 101-117.
816 <http://dx.doi.org/10.1016/j.envres.2012.03.013>

817 Mason, R.P., Fitzgerald, W.F., 1993. The distribution and biogeochemical cycling of mercury
818 in the equatorial Pacific Ocean. Deep Sea Research Part I: Oceanographic Research
819 Papers 40, 1897–1924. [https://doi.org/10.1016/0967-0637\(93\)90037-4](https://doi.org/10.1016/0967-0637(93)90037-4)

820 Mauchline, J., 1959. The biology of the euphausiid Crustacean, *Meganctiphanes norvegica*
821 (M. Sars). Proc. Roy. Soc. Edinb. B Biol. Sci. 67 (2), 141–179.

822 Michener, R.H., Kaufman, L., 2007. Stable isotope ratios as tracers in marine food webs: an
823 update. In: Michener, R.H., Lajtha, K. (Eds.), Stable Isotopes in Ecology and
824 Environmental Science, second ed. Blackwell, Malden, MA, pp. 238–282. 2007.

825 Minagawa, M., Wada, E., 1984. Stepwise enrichment of ^{15}N along food chains: further
826 evidence and the relation between $\delta^{15}\text{N}$ and animal age. Geochem. Cosmochim. Acta

827 48, 1135–1140.

828 Monteiro, L., Granadeiro, J., Furness, R., 1998. Relationship between mercury levels and diet
829 in Azores seabirds. *Marine Ecology Progress Series* 166, 259–265.
830 <https://doi.org/10.3354/meps166259>

831 Monteiro, L., Costa, V., Furness, R., Santos, R., 1996. Mercury concentrations in prey fish
832 indicate enhanced bioaccumulation in mesopelagic environments. *Marine Ecology
833 Progress Series* 141, 21–25. <https://doi.org/10.3354/meps141021>

834 Navarro, J., Coll, M., Somes, C.J., Olson, R.J., 2013. Trophic niche of squids: Insights from
835 isotopic data in marine systems worldwide. *Deep Sea Research Part II: Topical
836 Studies in Oceanography* 95, 93–102. <https://doi.org/10.1016/j.dsr2.2013.01.031>

837 Nigmatullin, Ch. M., 2004. Estimation of biomass, production and fishery potential of
838 *Ommastrephid* squids in the World Ocean and problems of their fishery forecasting.
839 ICES CM 2004 / CC: 06-14 p.

840 Noyon, M., Morris, T., Walker, D., Huggett, J., 2019. Plankton distribution within a young
841 cyclonic eddy off south-western Madagascar. *Deep Sea Res. II.* 166, 141-150.
842 <https://doi.org/10.1016/j.dsr2.2018.11.001>.

843 Padalkar, P.P., Chakraborty, P., Chennuri, K., Jayachandran, S., Sitlhou, L., Nanajkar, M.,
844 Tilvi, S., Singh, K., 2019. Molecular characteristics of sedimentary organic matter in
845 controlling mercury (Hg) and elemental mercury (Hg⁰) distribution in tropical
846 estuarine sediments. *Science of the Total Environment* 668, 592-601.
847 <https://doi.org/10.1016/j.scitotenv.2019.02.353>

848 Pakhomov, E.A., Perissinotto, R., McQuaid, C.D., 1996. Prey composition and daily rations
849 of myctophid fishes in the Southern Ocean. *Mar. Ecol. Prog. Ser.* 134, 1–14.

850 Parks, J.M., Johs, A., Podar, M., Bridou, R., Hurt Jr., R.A., Smith, S.D., Tomanicek, S.J.,
851 Qian, Y., Brown, S.D., Brandt, C.C., Palumbo, A.V., Smith, J.C., Wall, J.D., Elias,
852 D.A., Liang, L., 2013. The Genetic Basis for Bacterial Mercury Methylation. *Science*
853 339, 1332-1335.

854 Pearcy, W.G., Krygier, E.E., Mesecar, R., Ramsey, F., 1977. Vertical distribution and
855 migration of oceanic micronekton off Oregon. *Deep Sea Research* 24, 223–245.
856 [https://doi.org/10.1016/S0146-6291\(77\)80002-7](https://doi.org/10.1016/S0146-6291(77)80002-7)

857 Pellegrini, D., Barghigiani, C., 1989. Feeding behaviour and mercury content in two flat fish
858 in the northern Tyrrhenian sea. *Marine Pollution Bulletin* 20, 443–447.
859 [https://doi.org/10.1016/0025-326X\(89\)90064-7](https://doi.org/10.1016/0025-326X(89)90064-7)

860 Pinet, P., Jaquemet, S., Phillips, R. A., Le Corre, M., 2012. Sex-specific foraging strategies
861 throughout the breeding season in a tropical, sexually monomorphic small petrel.
862 *Animal Behaviour*, 83(4), 979-989. <https://doi.org/10.1016/j.anbehav.2012.01.019>

863 Post, D.M., Layman, C. A., Arrington, D. A., Takimoto, G., Quattrochi, J., Montana, C. G.,
864 2007. Getting to the fat of the matter: models, methods and assumptions for dealing
865 with lipids in stable isotope analyses. *Oecologia*, 152(1), 179-189.

866 Post, D.M., 2002. Using stable isotopes to estimate trophic position: Models, Methods, and
867 Assumptions. *Ecology* 83, 703–718. [https://doi.org/10.1890/0012-9658\(2002\)083\[0703:USITET\]2.0.CO;2](https://doi.org/10.1890/0012-9658(2002)083[0703:USITET]2.0.CO;2)

868

869 Potier, M., Marsac, F., Cherel, Y., Lucas, V., Sabatié, R., Maury, O., Ménard, F., 2007.
870 Forage fauna in the diet of three large pelagic fishes (lancetfish, swordfish and
871 yellowfin tuna) in the western equatorial Indian Ocean. *Fisheries Research* 83, 60–72.
872 <https://doi.org/10.1016/j.fishres.2006.08.020>

873 Proud, R., Handegard, N. O., Kloser, R. J., Cox, M. J., Brierley, A. S., 2018. From
874 siphonophores to deep scattering layers: uncertainty ranges for the estimation of
875 global mesopelagic fish biomass. *ICES Journal of Marine Science.* 76(3): 718-733.
876 <https://doi.org/10.1093/icesjms/fsy037>

- 877 Queirós, J. P., Bustamante, P., Cherel, Y., Coelho, J. P., Seco, J., Roberts, J., Pereira, E.,
878 Xavier, J. C., 2020. Cephalopod beak sections used to trace mercury levels throughout
879 the life of cephalopods: The giant warty squid *Moroteuthopsis longimana* as a case
880 study. *Marine Environmental Research*, 161.
881 <https://doi.org/10.1016/j.marenvres.2020.105049>
- 882 Ranchou-Peyruse, M., Monperrus, M., Bridou, R., Duran, R., Amouroux, D., Salvado, J.C.,
883 Guyoneaud, R., 2009. Overview of Mercury Methylation Capacities among
884 Anaerobic Bacteria Including Representatives of the Sulphate-Reducers: Implications
885 for Environmental Studies. *Geomicrobiology Journal* 26(1): 1-8. DOI:
886 10.1080/01490450802599227
- 887 Receveur, A., Vourey, E., Lebourges-Dhaussy, A., Menkes, C., Ménard, F., Allain, V., 2020.
888 Biogeography of micronekton assemblages in the Natural Park of the Coral Sea.
889 *Frontiers in Marine Science*, 7(449), 1–20. <https://doi.org/10.3389/fmars.2020.00449>
- 890 Robison, B.H., 1984. Herbivory by the myctophid fish *Ceratoscopelus warmingii*. *Marine*
891 *Biology* 84, 119–123. <https://doi.org/10.1007/BF00392995>
- 892 Romanov, E. V, Nikolic, N., Dhurmeea, Z., Bodin, N., Puech, A., Norman, S., Hollanda, S.,
893 Bourjea, J., West, W., Potier, M., 2020. Trophic ecology of albacore tuna (*Thunnus*
894 *alalunga*) in the western tropical Indian Ocean and adjacent waters. *Marine and*
895 *Freshwater Research*, 71(11), 1517–1542. <https://doi.org/10.1071/MF19332>
- 896 Romero-Romero, S., Choy, C.A., Hannides, C.C.S., Popp, B.N., Drazen, J.C., 2019.
897 Differences in the trophic ecology of micronekton driven by diel vertical migration.
898 *Limnol. Oceanogr.* 1–11. <https://doi.org/10.1002/lno.11128>.
- 899 Rubenstein, D.R., Hobson, K.A., 2004. From birds to butterflies: animal movement patterns
900 and stable isotopes. *Trends Ecol. Evol.* 19 (5), 256–263.
- 901 Ryan, C., McHugh, B., Trueman, C.N., Harrod, C., Berrow, S.D., O’Connor, I., 2012.
902 Accounting for the effects of lipids in stable isotope ($\delta^{13}\text{C}$ and $\delta^{15}\text{N}$ values) analysis
903 of skin and blubber of balaenopterid whales: Lipid extraction in stable isotope
904 analysis of whale skin and blubber. *Rapid Communications in Mass Spectrometry* 26,
905 2745–2754. <https://doi.org/10.1002/rcm.6394>
- 906 Shapiro, S.S., Wilk, M.B., 1965. An analysis of variance test for normality (complete
907 samples). *Biometrika* 52, 591–611. <https://doi.org/10.2307/2333709>.
- 908 Smith, M.M., Heemstra, P.C., 1986. *Smith’s Sea Fishes*. J.L.B. Smith Institute of
909 Ichthyology, Grahamstown, South Africa, p. 1047.
- 910 Storelli, M.M., Giacomini-Stuffler, R., Storelli, A., Marcotrigiano, G.O., 2005.
911 Accumulation of mercury, cadmium, lead and arsenic in swordfish and bluefin tuna
912 from the Mediterranean Sea: A comparative study. *Marine Pollution Bulletin* 50,
913 1004–1007. <https://doi.org/10.1016/j.marpolbul.2005.06.041>
- 914 Sutton, T.T., 2013. Vertical ecology of the pelagic ocean: classical patterns and new
915 perspectives. *J. Fish. Biol.* 83, 1508–1527. <https://doi.org/10.1111/jfb.12263>.
- 916 Tanaka, H., Ohshimo, S., Sassa, C., Aoki, I., 2007. Feeding Habits of Mesopelagic Fishes off
917 the Coast of Western Kyushu. *PICES 16th: Bio, Japan*, p. 4200, 1st November.
- 918 Tew-Kai, E., Marsac, F., 2009. Patterns of variability of sea surface chlorophyll in the
919 Mozambique Channel: a quantitative approach. *J. Mar. Syst.* 77 (1–2), 77–88.
920 <https://doi.org/10.1016/j.jmarsys.2008.11.007>.
- 921 Topping, G., Davies, I.M., 1981. Methylmercury production in the marine water column.
922 *Nature* 290, 243–244. <https://doi.org/10.1038/290243a0>
- 923 van der Spoel, S., Bleeker, J., 1991. Distribution of Myctophidae (pisces, myctophiformes)
924 during the four seasons in the mid north atlantic. *Contrib. Zool.* 61(2), 89–106.
- 925 Vanderklift, M.A., Ponsard, S., 2003. Sources of variation in consumer-diet $\delta^{15}\text{N}$ enrichment:
926 a meta-analysis. *Oecologia* 136 (2), 169–182.

- 927 Vianello, P., Ternon, J-F., Demarcq, H., Herbette, S., Roberts, M.J., 2020. Ocean currents
928 and gradients of surface layer properties in the vicinity of the Madagascar Ridge
929 (including seamounts) in the South West Indian Ocean. *Deep Sea Res II*, 176, 104816.
930 <https://doi.org/10.1016/j.dsr2.2020.104816>
- 931 Watras, C.J., Back, R.C., Halvorsen, S., Hudson, R.J.M., Morrison, K.A., Wentz, S.P., 1998.
932 Bioaccumulation of mercury in pelagic freshwater food webs. *Science of The Total*
933 *Environment* 219, 183–208. [https://doi.org/10.1016/S0048-9697\(98\)00228-9](https://doi.org/10.1016/S0048-9697(98)00228-9)
- 934 Young, J.W., Hunt, B.P.V., Cook, T.R., Llopiz, J.K., Hazen, E.L., Pethybridge, H.R.,
935 Ceccarelli, D., Lorrain, A., Olson, R.J., Allain, V., Menkes, C., Patterson, T., Nicol,
936 S., Lehodey, P., Kloser, R.J., Arrizabalaga, H., Anela Choy, C., 2015. The
937 trophodynamics of marine top predators: Current knowledge, recent advances and
938 challenges. *Deep Sea Research Part II: Topical Studies in Oceanography* 113, 170–
939 187. <https://doi.org/10.1016/j.dsr2.2014.05.015>
- 940 Zhang, Y., Soerensen, A. L., Schartup, A. T., Sunderland, E. M., 2020. A global model for
941 methylmercury formation and uptake at the base of marine food webs. *Global*
942 *Biogeochemical Cycles*, 34(2), e2019GB006348.

943

944 **List of figures**

945 Fig. 1(a) Map of the south-western Indian Ocean showing the trawl stations conducted at two
946 seamounts (La Pérouse and MAD-Ridge) and the open ocean investigation at Reunion Island
947 and Mozambique Channel (MZC). Longhurst's (1998) biogeochemical provinces are
948 delimited by black solid lines and are labelled as EAFR (East African Coastal Province) and
949 ISSG (Indian South Subtropical Gyre). The western African, Madagascar and Mascarene
950 landmasses are shown in grey. A 3D-bathymetry of (b) La Pérouse and (c) MAD-Ridge
951 seamounts. Colour bar represents the depth (m) below the sea surface.

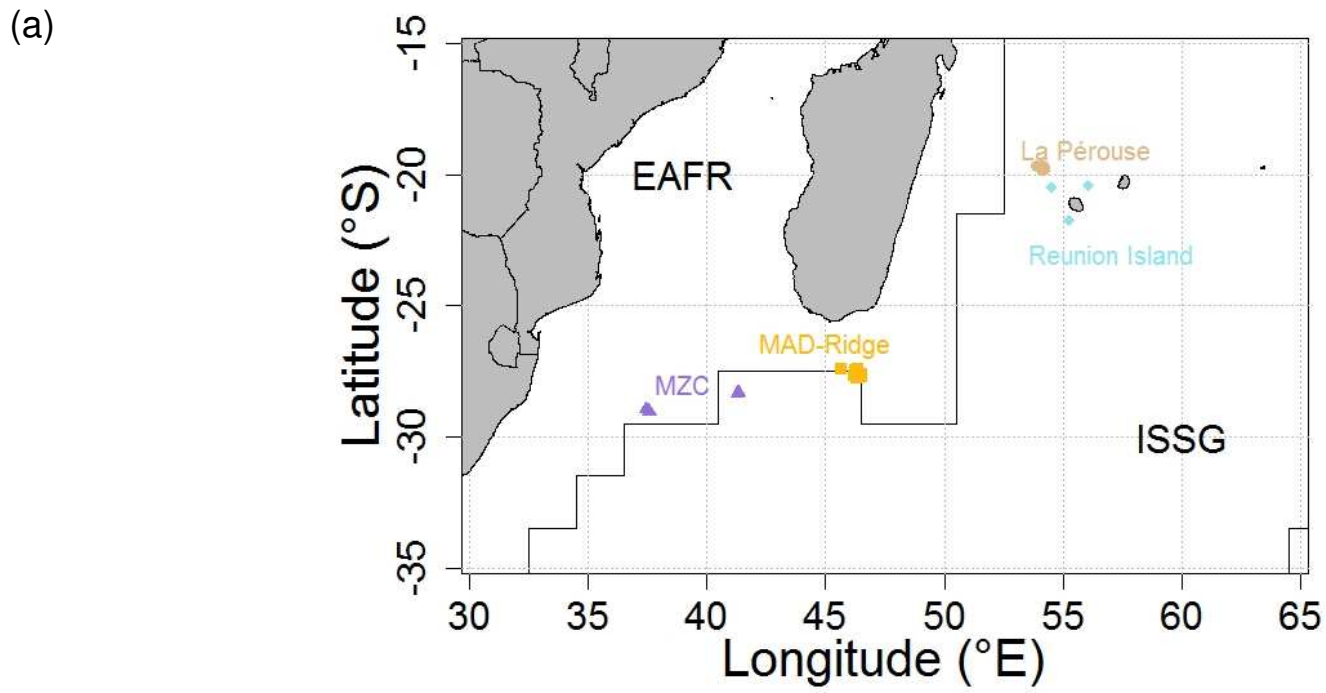
952 Fig. 2(a) Averaged satellite image of sea surface chlorophyll *a* concentrations from
953 18/09/2016 to 07/12/2016 at the La Pérouse and MAD-Ridge seamounts (represented by
954 black star symbols) in the south-western Indian Ocean. Colour bar indicates the surface mean
955 concentrations in mg m^{-3} . (b) Averaged mean sea level anomaly (MSLA) map, with La
956 Pérouse and MAD-Ridge seamounts shown as black star symbols, and dated 14–23
957 November 2016. Colour bar indicates the SLA in cm, with positive SLA (red) and negative
958 SLA (blue).

959 Fig. 3 Boxplots of mercury (Hg) concentrations ($\mu\text{g g}^{-1}$ dw) in (a) the most common
960 crustacean and fish families from the study sites (La Pérouse, $n= 32$; MAD-Ridge, $n= 72$;
961 Mozambique Channel-MZC, $n= 28$; Reunion Island, $n= 40$), (b) micronekton from all study
962 sites, (c) the broad categories (Crustaceans, Fishes and Squids), (d) selected taxa according to
963 the minimum and maximum habitat ranges of the identified species (Epipelagic-Mesopelagic,
964 $n= 9$; Mesopelagic, $n= 178$; Mesopelagic-Bathypelagic, $n= 79$; Mesopelagic-Benthopelagic,
965 $n= 3$), (e) selected taxa according to feeding mode (carnivorous and omnivorous) from the
966 four study sites. The median (thick black line in box plots), interquartile range (the lower and
967 upper boundaries), the spread (thin lines extending from box plots) and outliers (black stars)
968 are shown.

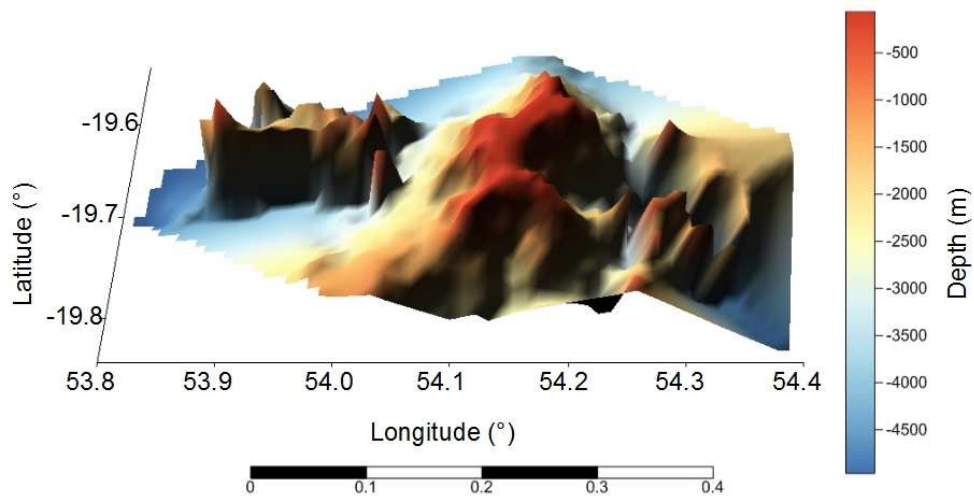
969 Fig. 4 Mercury (Hg) concentrations ($\mu\text{g g}^{-1}$ dw) in selected taxa *vs* body size (abdomen and
970 carapace length for crustaceans, standard length for fishes and dorsal mantle length for
971 squids) in mm, from the different study sites (La Pérouse, MAD-Ridge, Mozambique
972 Channel, and Reunion Island). The data from Mozambique Channel and Reunion Island fit a
973 linear curve (regression equations are given) but no relationship were found between Hg
974 concentrations and nekton body size at La Pérouse and MAD-Ridge seamounts.

975 Fig. 5 Boxplots of $\delta^{15}\text{N}$ and $\delta^{13}\text{C}$ stable isotope values in selected taxa from the study sites
976 (La Pérouse, $n= 30$; MAD-Ridge, $n= 97$; Mozambique Channel-MZC, $n= 30$). The median
977 (thick black line in box plots), mean (diamond symbols), interquartile range (the lower and
978 upper boundaries), the spread (thin lines extending from box plots) and outliers (red stars) are
979 shown.

980 Fig. 6 Mercury (Hg) concentrations ($\mu\text{g g}^{-1}$ dw) in selected taxa *vs* $\delta^{13}\text{C}$ and $\delta^{15}\text{N}$ stable
981 isotope values (‰) from the study sites (La Pérouse, MAD-Ridge and Mozambique
982 Channel). The data ($\delta^{15}\text{N}$ values) from MAD-Ridge and the Mozambique Channel fit
983 exponential curves. No significant relationships were found between Hg concentrations and
984 $\delta^{13}\text{C}$ values at La Pérouse, MAD-Ridge seamounts and the Mozambique Channel, and
985 between Hg and $\delta^{15}\text{N}$ values at La Pérouse.



(b)
La Pérouse seamount



(c)
MAD-Ridge seamount

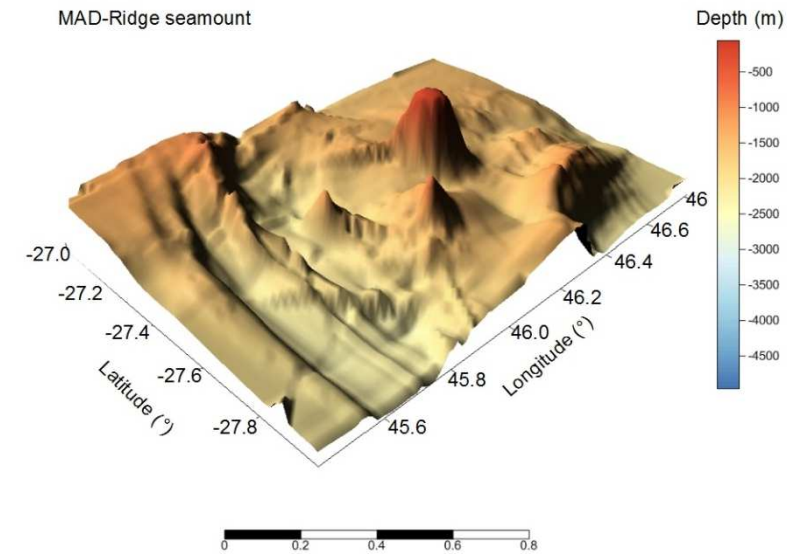
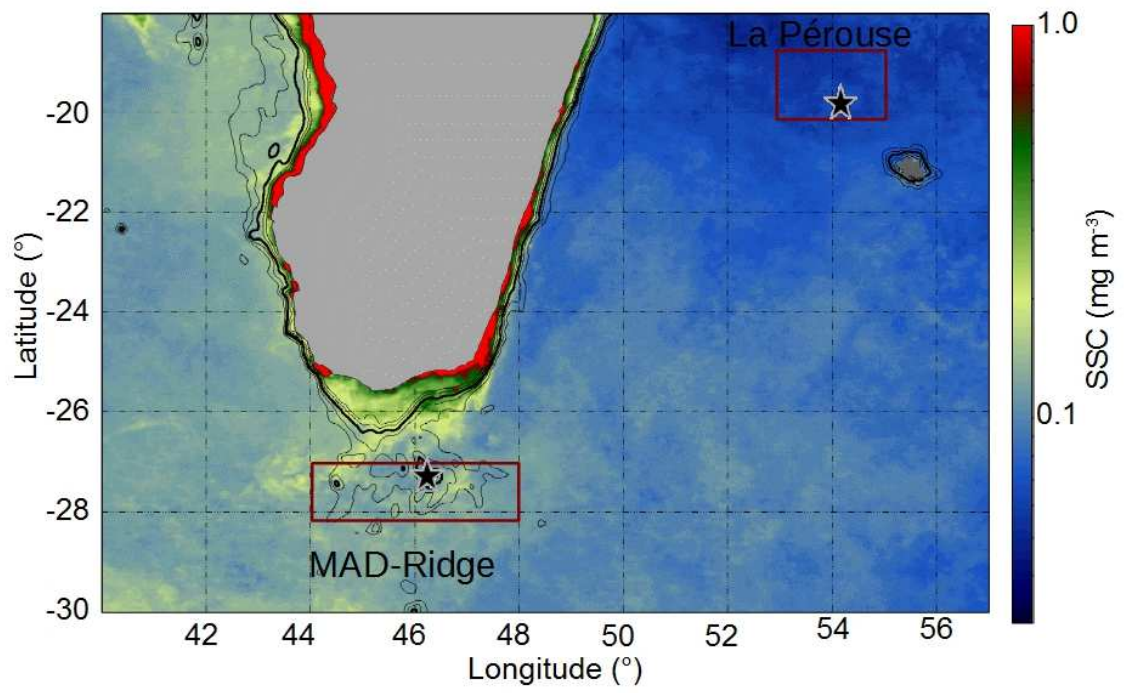


Figure 1

(a)



(b)

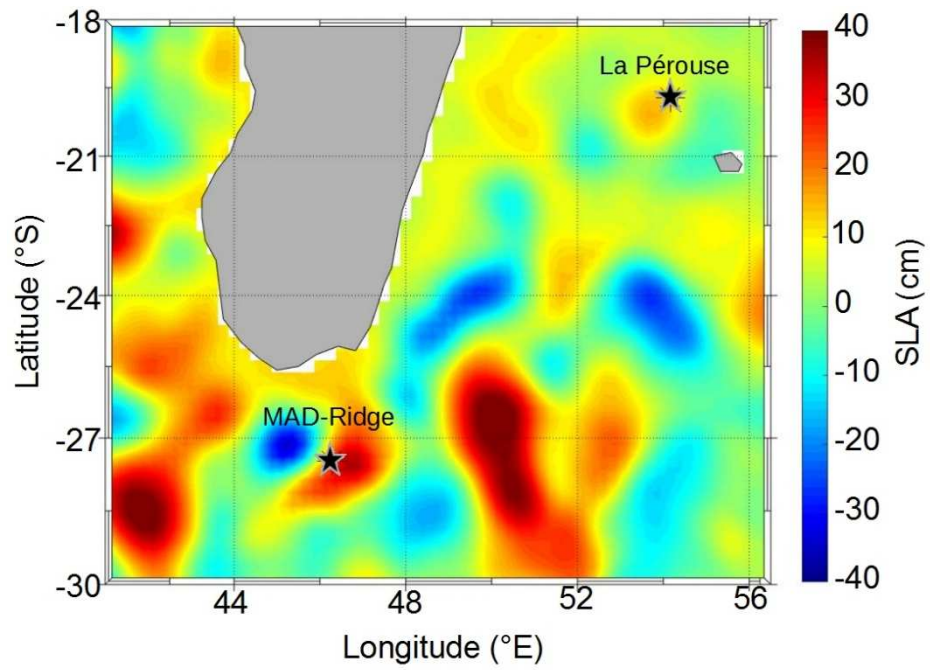


Figure 2

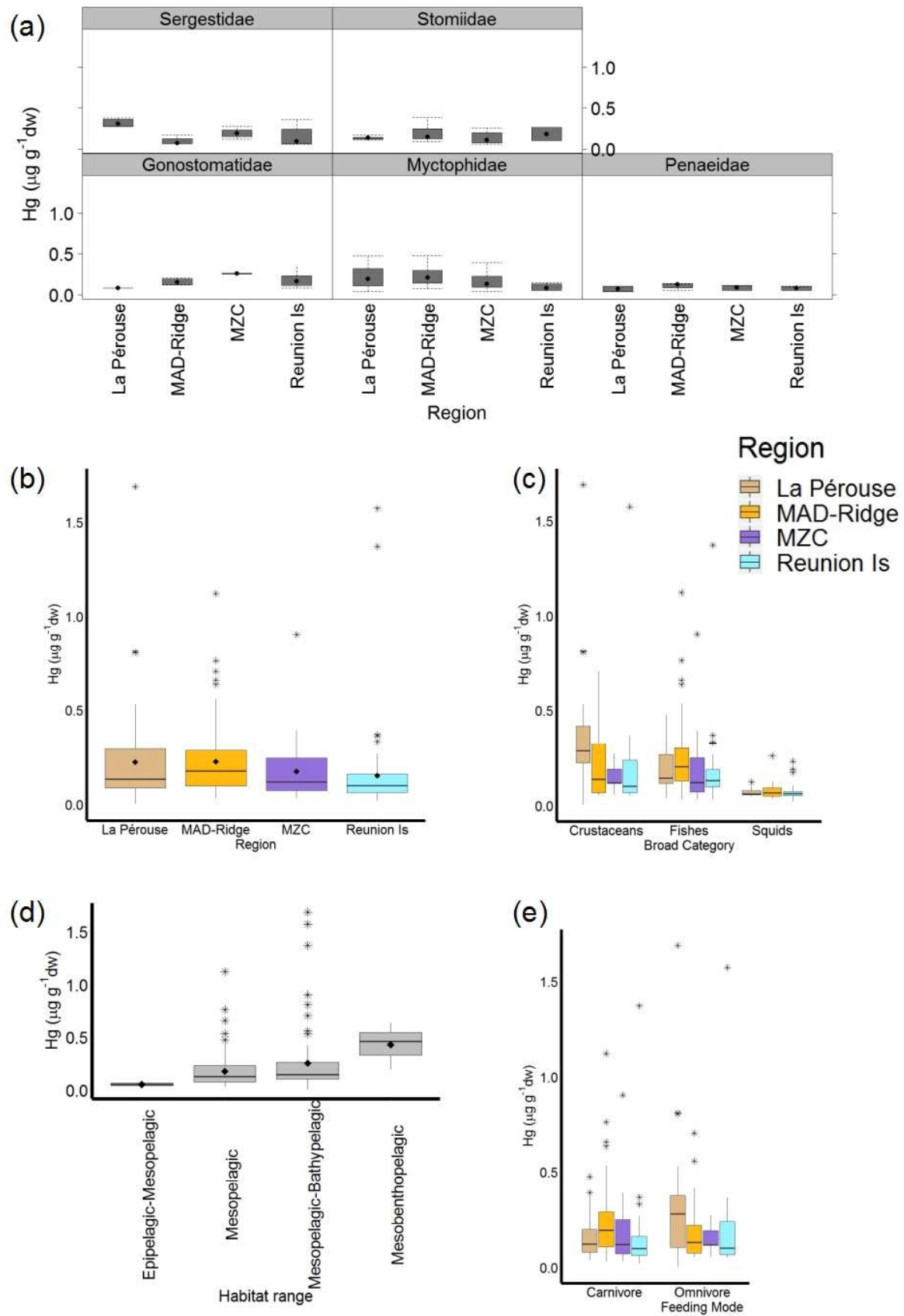


Figure 3

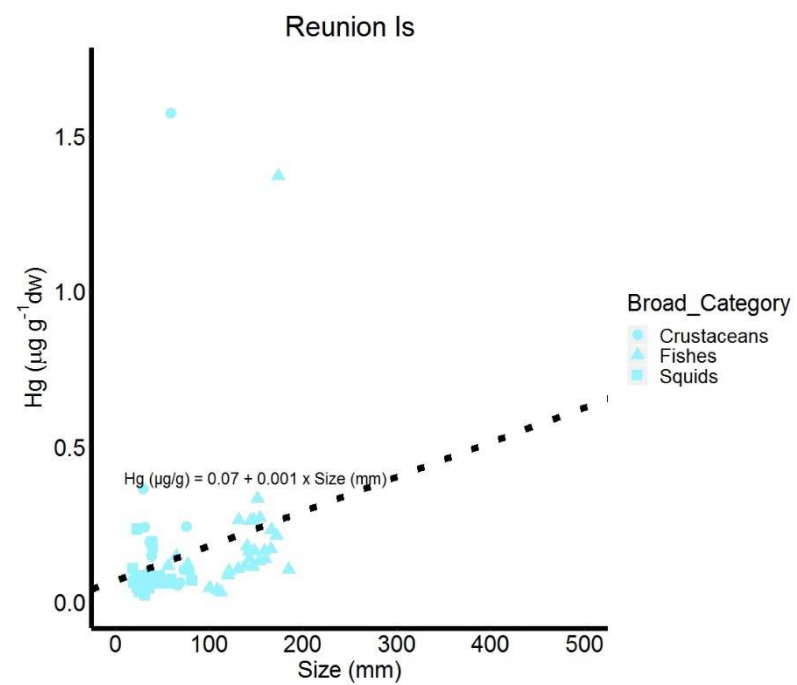
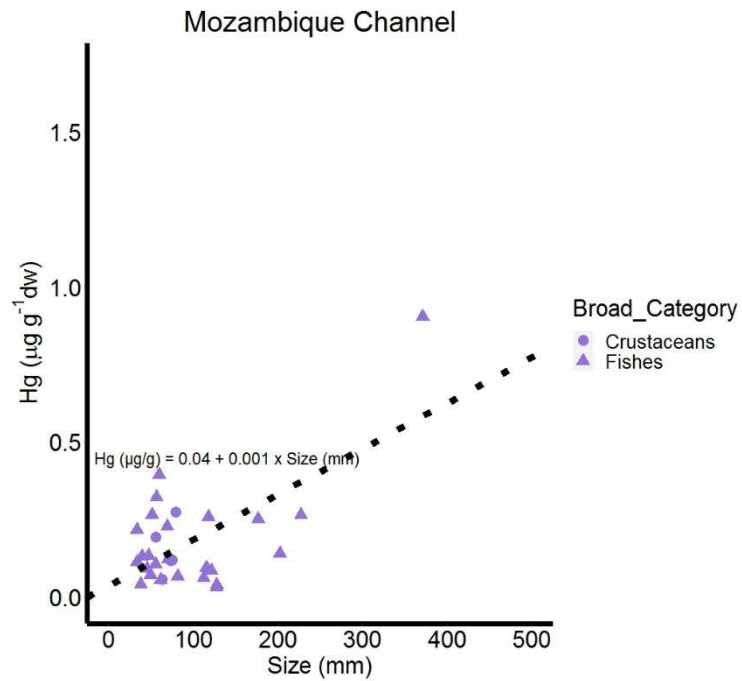
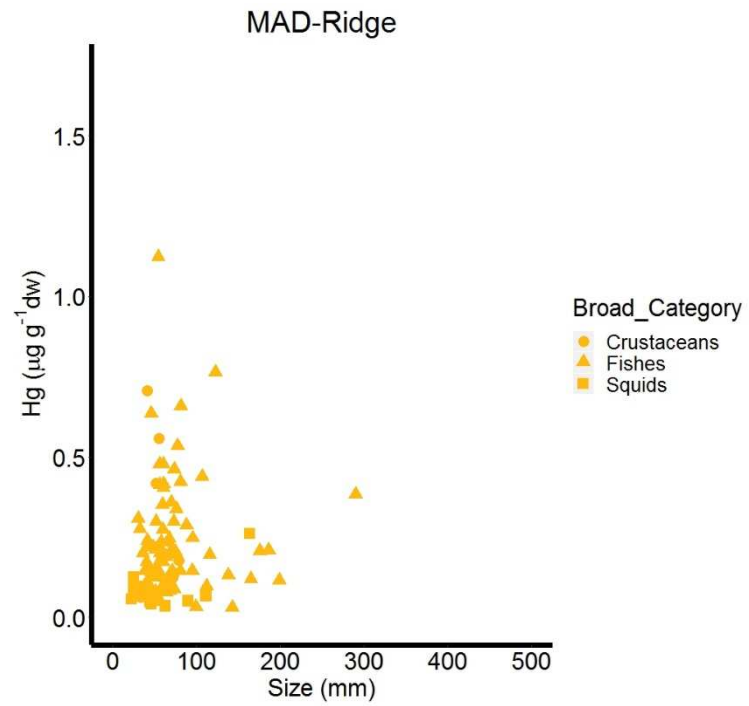
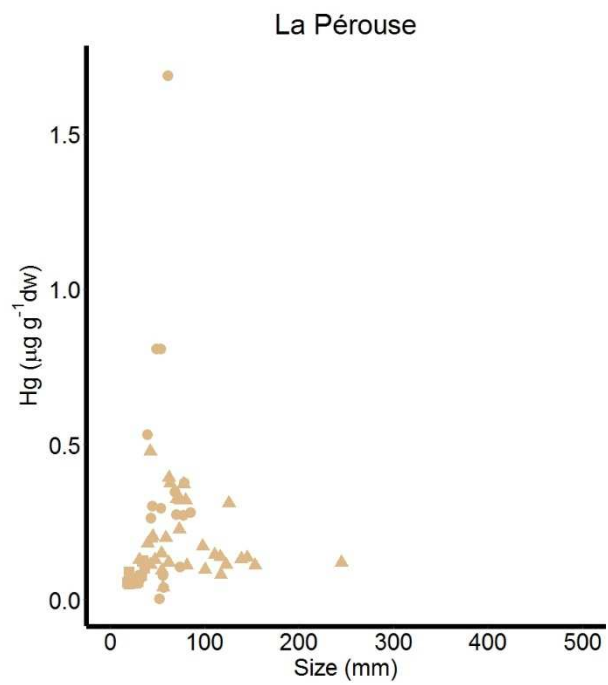


Figure 4

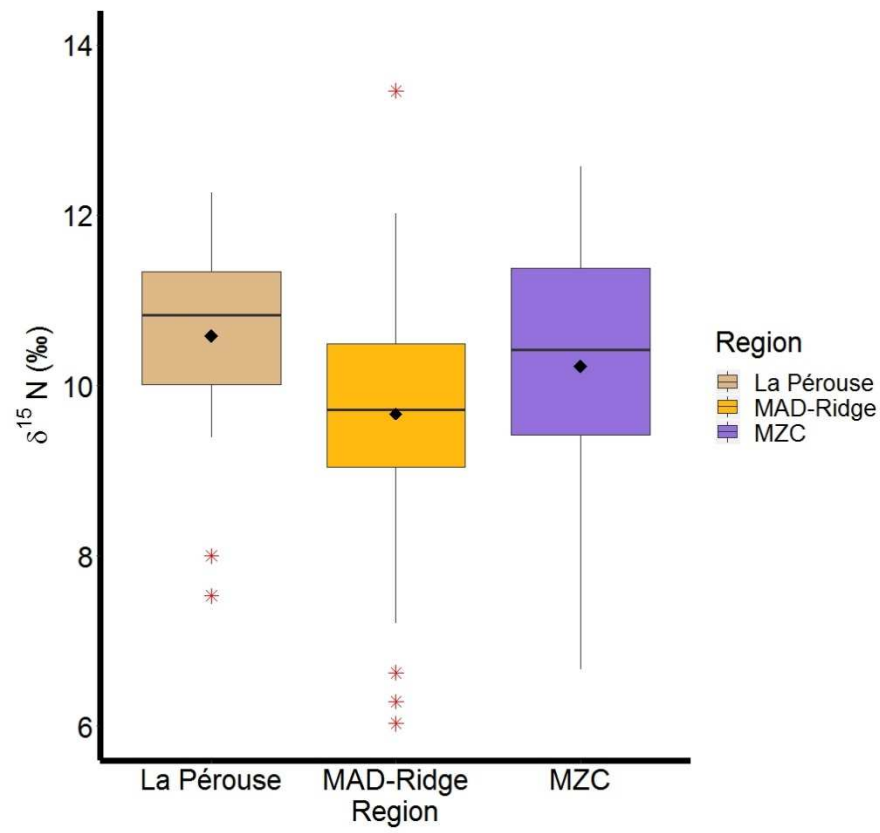
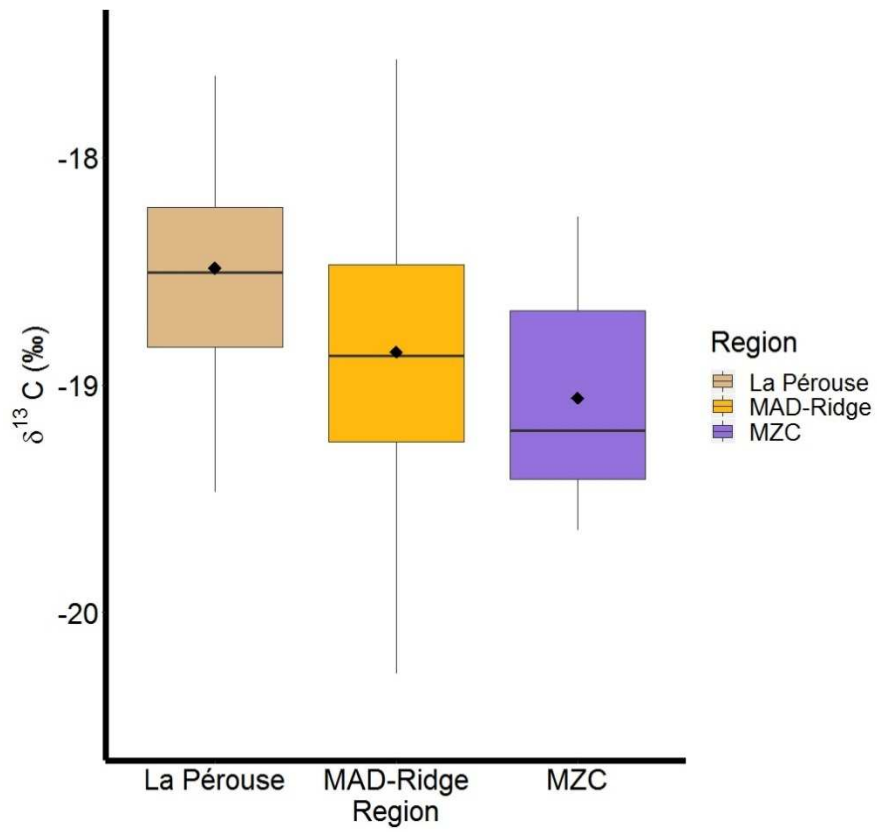


Figure 5

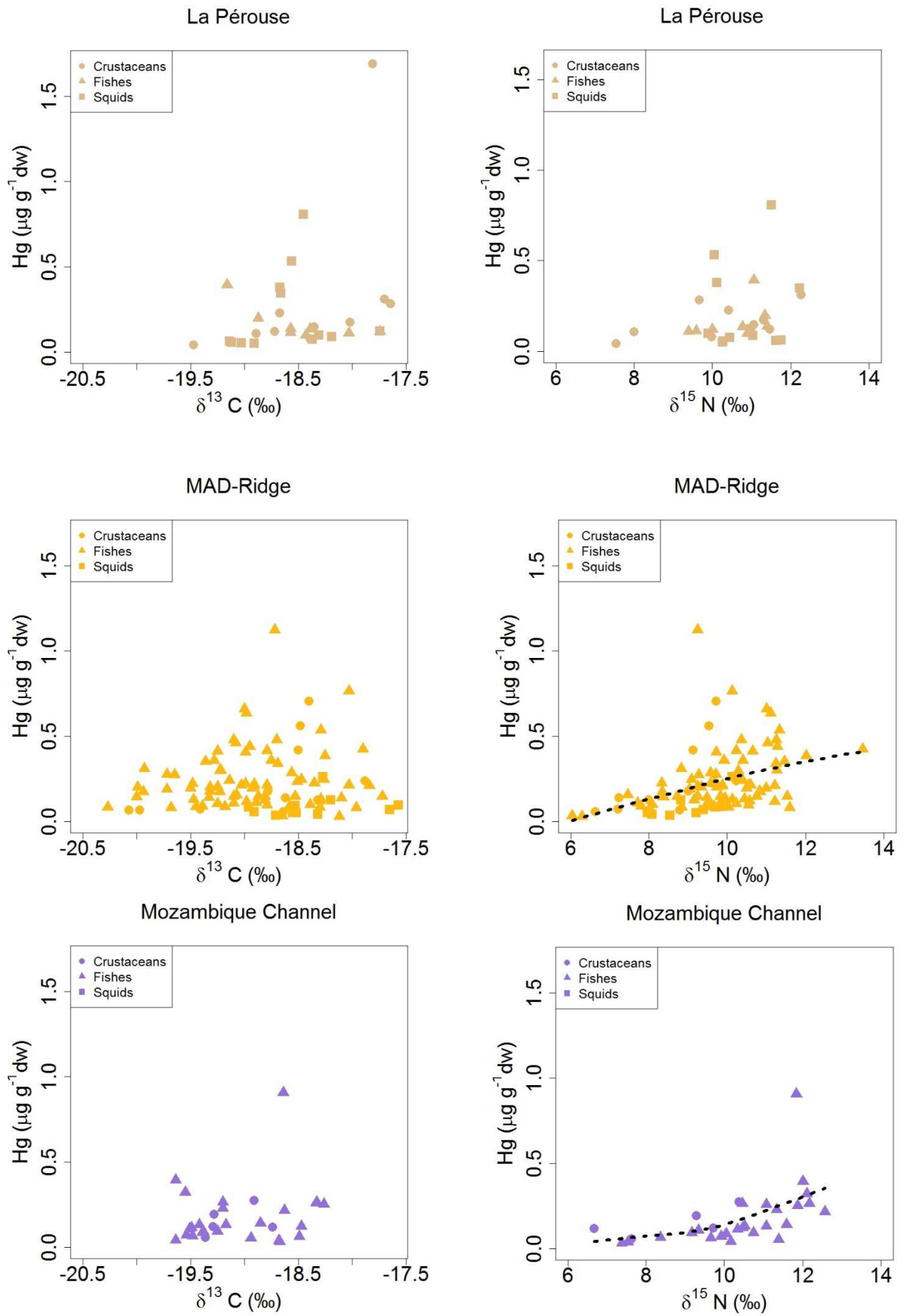


Figure 6

Table 1. Mean body length (mm) of crustaceans (abdomen and carapace length); squids (dorsal mantle length); fishes (standard length), total number of specimens (n), habitat range and feeding mode obtained from literature, $\delta^{15}\text{N}$ and $\delta^{13}\text{C}$ (‰), mean mercury (Hg) concentrations ($\mu\text{g g}^{-1}$ dw) and mean estimated trophic level (Mean TL) for the species or taxa on which stable isotope analyses were performed at La Pérouse (ISSG) and MAD-Ridge (EAFR) seamounts, the south-western Mozambique Channel (MZC) and Reunion Island. Values are mean \pm standard deviation.

Order, Suborder, Infraorder, Superfamily	Family / Species	Habitat	Feeding Mode	Region	Trawl No.	n	Size range (mm)	Mean Size (mm)	Mean $\delta^{15}\text{N}$ (‰)	Mean $\delta^{13}\text{C}$ (‰)	Mean Hg ($\mu\text{g g}^{-1}$ dw)	Mean TL
Crustaceans												
Decapoda												
Pleocyemata	Oplophoridae	Mesopelagic	Omnivore	La Pérouse	1, 7	8	39-61	49.3 \pm 7.03	10.9 \pm 0.79	-18.3 \pm 0.41	0.59 \pm 0.53	3.8 \pm 0.25
Caridea		- Bathypelagic		MAD-Ridge	1, 2, 5	4	41-67	53.6 \pm 10.7	9.7 \pm 0.46	-18.3 \pm 0.29	0.48 \pm 0.20	3.7 \pm 0.14
				Reunion Is	1	4	31-59	41.4 \pm 12.3			0.54 \pm 0.69	
	Pasiphaeidae											
	<i>Pasiphaea</i> spp.	Mesopelagic - Bathypelagic	Omnivore	La Pérouse	9	2	56-85	70.4 \pm 20.5	9.8 \pm 0.23	-18.0 \pm 0.53	0.18 \pm 0.14	3.4 \pm 0.07
Dendrobranchiata	Penaeidae											
Penaeoidea												
	<i>Funchalia</i> sp.	Mesopelagic - Bathypelagic	Omnivore	La Pérouse	8	2	56-74	64.8 \pm 12.3	7.8 \pm 0.33	-19.2 \pm 0.41	0.07 \pm 0.05	2.8 \pm 0.10
				MAD-Ridge	5, 6	3	54-74	66.4 \pm 10.7	7.3 \pm 0.68	-18.5 \pm 0.18	0.11 \pm 0.04	3.0 \pm 0.21
				MZC	21	2	63-74	68.6 \pm 7.42	7.2 \pm 0.68	-19.1 \pm 0.44	0.09 \pm 0.04	2.9 \pm 0.21
				Reunion Is	1	4	67-79	71.7 \pm 5.16			0.08 \pm 0.02	
Sergestoidea	Sergestidae	Mesopelagic	Omnivore	La Pérouse	2	4	68-78	73.5 \pm 5.21	11.2 \pm 1.50	-18.7 \pm 0.01	0.32 \pm 0.05	3.8 \pm 0.47

MAD-Ridge	2	4	33-79	50.8 ± 19.4	8.3 ± 0.82	-19.6 ± 0.59	0.09 ± 0.06	3.3 ± 0.26
MZC	18	3	56-79	69.9 ± 12.6	9.8 ± 0.54	-19.2 ± 0.22	0.20 ± 0.08	3.7 ± 0.17
Reunion Is	1	5	30-76	50.5 ± 18.1			0.17 ± 0.13	

Order	Family / Species	Habitat	Feeding Mode	Region	Trawl No.	n	Size range (mm)	Mean Size (mm)	Mean $\delta^{15}\text{N}$ (‰)	Mean $\delta^{13}\text{C}$ (‰)	Mean Hg ($\mu\text{g g}^{-1}$ dw)	Mean TL (TPA model)	
Squids													
Oegopsida	Enoploteuthidae	Mesopelagic-Bathypelagic	Carnivore	MAD-Ridge	11	2	22-46	34.1 ± 16.8	8.0 ± 0.06	-18.6 ± 0.42	0.05 ± 0.01	3.2 ± 0.02	
				Reunion Is	1, 3	7	21-39	27.2 ± 6.51		0.09 ± 0.05			
	<i>Abralia</i> sp.	Mesopelagic	Carnivore	Reunion Is	3, 5	4	20-30	26.4 ± 4.6			0.06 ± 0.01		
	<i>Abraliopsis</i> sp.	Mesopelagic-Bathypelagic	Carnivore	La Pérouse	3, 4, 6	11	18-36	28.1 ± 6.19	10.5 ± 0.45	-18.4 ± 0.48	0.07 ± 0.02	3.6 ± 0.14	
				MAD-Ridge	2, 9, 10	4	25-35	29.2 ± 4.95	9.5 ± 0.48	-18.3 ± 0.59	0.10 ± 0.02	3.6 ± 0.15	
				Reunion Is	1	1	29.2	29.2		0.06			
	Histioteuthidae												
	<i>Histioteuthis</i> spp.	Mesopelagic	Carnivore	La Pérouse	9	2	28.9-29.4	29.2 ± 0.35	11.7 ± 0.10	-19.1 ± 0.01	0.06 ± 0.002	4.0 ± 0.03	
				Reunion Is	1, 3	4	19-47	35.0 ± 14.6		0.08 ± 0.02			
	Ommastrephidae												
<i>Ornithoteuthis volatilis</i>	Mesopelagic	Carnivore	MAD-Ridge	12, 14, 16	4	45-163	90.1 ± 52.2	9.0 ± 0.93	-18.5 ± 0.18	0.10 ± 0.11	3.5 ± 0.29		
<i>Sthenoteuthis oualaniensis</i>	Mesopelagic	Carnivore	Reunion Is	1	3	33-40	36.5 ± 3.5			0.09 ± 0.08			
<i>Ommastrephes bartramii</i>	Mesopelagic	Carnivore	MAD-Ridge	1	1		364.8	13.2	-17.4	0.82	4.8		
			MZC	20	1		489.8	13.8	-17.3	0.92	5.0		
<i>Euclideanoteuthis luminosa</i>	Mesopelagic	Carnivore	MAD-Ridge	2	1	111.3	111.3	9.4	-17.7	0.07	3.6		
Onychoteuthidae													
<i>Onychoteuthis</i> sp.	Epipelagic-Mesopelagic	Carnivore	Reunion Is	1, 3, 5	9	24-82	37.0 ± 20.1			0.05 ± 0.02			
Pyroteuthidae													

Pyroteuthis sp.

Mesopelagic

Carnivore

Reunion Is

1

2

23

23.4 ± 0.0

0.14 ± 0.13

Order/ Suborder/Infraorder	Family/ Species	Habitat Range	Feeding Mode	Region	Trawl No.	n	Size range (mm)	Mean Size (mm)	Mean $\delta^{15}\text{N}$ (‰)	Mean $\delta^{13}\text{C}$ (‰)	Mean Hg (μg g^{-1} dw)	Mean TL
Fishes												
Beryciformes	Diretmidae											
	<i>Diretmus argenteus</i>	Mesopelagic	Carnivore	MAD-Ridge	7	1	30.3	30.3	8.82	-19.9	0.31	3.4
Myctophiformes	Neosopelidae											
	<i>Neosopelus macrolepidotus</i>	Mesopelagic- Benthopelagic over slope regions	Carnivore	MAD-Ridge	10	2	46-116	80.9 ± 49.3	10.8 ± 0.44	-19.2 ± 0.37	0.42 ± 0.31	4.1 ± 0.14
	<i>Neosopelus microchir</i>	Mesopelagic- Benthopelagic over slope regions	Carnivore	MAD-Ridge	10	1	73.4	73.4	11.0	-19.1	0.46	4.1
	Myctophidae											
	<i>Benthoosema fibulatum</i>	Mesopelagic	Carnivore	MAD-Ridge	14	2	70-88	79.1 ± 12.8	9.75 ± 0.25	-18.7 ± 0.13	0.32 ± 0.05	3.7 ± 0.08
	<i>Bolinichthys photothorax</i>	Mesopelagic	Carnivore	La Pérouse	10	2	62-73	67.5 ± 7.78	10.9 ± 0.74	-18.7 ± 0.04	0.17 ± 0.08	3.8 ± 0.23
	<i>Ceratoscopelus warmingii</i>	Mesopelagic	Omnivore	La Pérouse	8	1	54.8	54.8			0.09	
				MAD-Ridge	2, 3, 6	3	41-68	50.4 ± 15.5	8.0 ± 0.73	-18.8 ± 0.45	0.12 ± 0.04	3.2 ± 0.23
	Myctophidae sp.	Mesopelagic		Reunion Is	1	4	40-65	55.1 ± 10.7			0.09 ± 0.05	
	<i>Diaphus brachycephalus</i>	Mesopelagic	Carnivore	MAD-Ridge	5	1	40.4	40.4	10.8	-19.2	0.17	4.1
	<i>Diaphus diadematus</i>	Mesopelagic	Carnivore	MAD-Ridge	5	2	33-36	34.2 ± 2.40	9.52 ± 0.27	-19.9 ± 0.19	0.24 ± 0.05	3.7 ± 0.08
	<i>Diaphus effulgens</i>	Mesopelagic	Carnivore	MAD-Ridge	5	2	75-107	90.7 ± 22.5	10.3 ± 1.44	-19.1 ± 0.21	0.32 ± 0.16	3.9 ± 0.45
	<i>Diaphus knappi</i>	Mesopelagic	Carnivore	MAD-Ridge	16	2	45-61	53.1 ± 11.0	10.2 ± 0.07	-19.4 ± 0.16	0.12 ± 0.02	3.9 ± 0.02
	<i>Diaphus lucidus</i>	Mesopelagic	Carnivore	La Pérouse	10	3	74-80	77.2 ± 2.87			0.34 ± 0.03	
				MZC	20	1	69.2	69.2	11.3	-19.2	0.23	4.2
	<i>Diaphus metoclampus</i>	Mesopelagic	Carnivore	MZC	20	2	57-60	58.1 ± 2.12	12.1 ± 0.07	-19.6 ± 0.06	0.36 ± 0.05	4.4 ± 0.02
	<i>Diaphus mollis</i>	Mesopelagic	Carnivore	La Pérouse	10	2	40-47	43.5 ± 5.23			0.15 ± 0.04	
				MAD-Ridge	5, 7	3	46-59	53.9 ± 6.97	10.6 ± 1.01	-19.3 ± 0.02	0.22 ± 0.11	4.0 ± 0.32
	<i>Diaphus perspicillatus</i>	Mesopelagic	Carnivore	La Pérouse	10	3	42-62	53.5 ± 10.1	11.1	-19.2	0.18 ± 0.19	3.8
				MAD-Ridge	2, 5, 7, 9, 12	10	48-61	56.0 ± 4.59	10.2 ± 0.53	-19.1 ± 0.24	0.35 ± 0.10	3.9 ± 0.17
				MZC	21	2	51-61	56.2 ± 7.21	10.9 ± 0.66	-19.1 ± 0.18	0.16 ± 0.15	4.1 ± 0.21
	<i>Diaphus richardsoni</i>	Mesopelagic	Carnivore	MAD-Ridge	15	1	44.0	44.0	9.44	-19.5	0.09	3.6
				MZC	21	2	46-47	46.2 ± 0.92	10.9 ± 0.23	-19.3 ± 0.15	0.11 ± 0.03	4.1 ± 0.07
	<i>Diaphus suborbitalis</i>	Mesopelagic-over slope regions	Carnivore	La Pérouse	2	2	59-71	64.7 ± 8.20			0.26 ± 0.09	
				MAD-Ridge	10, 14, 17	5	64-81	72.7 ± 6.57	11.2 ± 0.25	-18.8 ± 0.49	0.31 ± 0.22	4.2 ± 0.08
	<i>Hygophum hygomii</i>	Mesopelagic	Carnivore	MAD-Ridge	2, 6, 12, 17	8	51-60	55.1 ± 3.50	9.95 ± 0.95	-19.2 ± 0.65	0.19 ± 0.06	3.8 ± 0.30
				MZC	21	2	49-55	52.4 ± 4.17	9.6 ± 0.41	-19.5 ± 0.02	0.09 ± 0.02	3.7 ± 0.13

	<i>Lampanyctus</i> sp.	Mesopelagic	Carnivore	La Pérouse	10	2	101-123	111.5 ± 15.6	10.2 ± 0.92	-18.5 ± 0.10	0.10 ± 0.01	3.5 ± 0.29
	<i>Lampanyctus alatus</i>	Mesopelagic	Carnivore	MAD-Ridge	3	2	38-43	40.5 ± 3.25	8.52 ± 0.28	-18.6 ± 0.33	0.19 ± 0.06	3.3 ± 0.09
	<i>Lobianchia dofleini</i>	Mesopelagic	Carnivore	MZC	20	1	33.6	33.6	12.6	-18.6	0.22	4.6
	<i>Lobianchia gemellarii</i>	Mesopelagic	Carnivore	La Pérouse	10	1	42.3	42.3			0.48	
				MAD-Ridge	5	1	41.5	41.5	10.3	-19.1	0.24	3.9
	<i>Myctophum fissunovi</i>	Mesopelagic	Carnivore	MAD-Ridge	6, 14	3	61-66	62.7 ± 2.70	9.84 ± 0.17	-19.2 ± 0.25	0.10 ± 0.01	3.8 ± 0.05
	<i>Myctophum nitidulum</i>	Mesopelagic	Carnivore	MAD-Ridge	6, 14	2	64-71	67.4 ± 4.88	9.5 ± 0.59	-19.3 ± 0.66	0.20 ± 0.02	3.6 ± 0.19
	<i>Notoscopelus resplendens</i>	Mesopelagic-Bathypelagic	Carnivore	MAD-Ridge	3	1	37.7	37.7	8.08	-18.4	0.10	3.2
				MZC	21	2	34-39	36.5 ± 4.10	10.4 ± 0.13	-19.5 ± 0.05	0.12 ± 0.01	3.9 ± 0.04
	<i>Scopelopsis multipunctatus</i>	Mesopelagic	Carnivore	MAD-Ridge	5	1	35.3	35.3	10.0	-20.3	0.08	3.8
				MZC	21	1	38.0	38.0	10.2	-19.6	0.04	3.9
Perciformes	Carangidae											
	<i>Decapterus macarellus</i>	Mesopelagic	Carnivore	MAD-Ridge	7	2	99-143	121 ± 30.5	6.16 ± 0.18	-18.4 ± 0.37	0.03 ± 0.002	2.6 ± 0.06
				MZC	21	2	128	127.6 ± 0.07	7.5 ± 0.11	-18.7 ± 0.01	0.04 ± 0.004	3.0 ± 0.03
				Reunion Is	5	3	101-113	107.3 ± 6.11			0.04 ± 0.01	
	Gempylidae											
	<i>Promethichthys prometheus</i>	Mesopelagic-Benthopelagic	Carnivore	MAD-Ridge	14	2	235.4-365	300 ± 91.5	12.0 ± 0.06	-17.9 ± 0.13	0.14 ± 0.02	4.4 ± 0.02
	Priacanthidae											
	<i>Cookeolus japonicus</i>	Mesopelagic-Benthopelagic	Carnivore	MAD-Ridge	16	2	207.9-328	268 ± 84.9	10.7 ± 0.47	-18.3 ± 0.35	0.25 ± 0.01	4.0 ± 0.15
	Scombrobracidae											
	<i>Scombrobrax heterolepis</i>			Reunion Is	1	2	77.1	77.1			0.14 ± 0.03	
Stomiiformes	Gonostomatidae											
	<i>Cyclothone</i> sp.	Mesopelagic-Bathypelagic	Carnivore	MAD-Ridge	7	1	59.9	59.9	8.34	-19.9	0.17	3.6
	<i>Sigmops elongatus</i>	Mesopelagic-Bathypelagic	Carnivore	La Pérouse	8	1	117.2	117.2			0.08	
				MAD-Ridge	2, 12	3	138-186	163.0 ± 24.2	10.7 ± 0.42	-18.1 ± 0.26	0.15 ± 0.05	4.0 ± 0.13
				MZC	20	2	177-227	201.8 ± 35.6	12.0 ± 0.21	-18.3 ± 0.05	0.26 ± 0.01	4.4 ± 0.07
				Reunion Is	1, 3, 5	25	120-174	148.9 ± 14.9			0.22 ± 0.25	
	Phosichthyidae											
	<i>Vinciguerria nimbaria</i>	Mesopelagic	Carnivore	La Pérouse	8	3	31-45	39.7 ± 7.73	11.3	-18.9	0.18 ± 0.04	3.9
	Sternoptychidae											
	<i>Argyropelecus aculeatus</i>	Mesopelagic	Carnivore	La Pérouse	7	2	54-63	58.9 ± 6.29			0.26 ± 0.16	
				MAD-Ridge	1, 2, 5, 12	4	54-81	66.6 ± 14.5	10.8 ± 2.0	-18.4 ± 0.42	0.55 ± 0.42	4.1 ± 0.64
				Reunion Is	1	3	19-38	30.6 ± 10.3			0.09 ± 0.01	
	Stomiidae											
	<i>Astronesthes</i> sp.	Mesopelagic	Carnivore	La Pérouse	10	1	81.2	81.2	9.4	-18.0	0.11	3.3
				MAD-Ridge	5	1	122.3	122.3	10.1	-18.0	0.76	3.8

<i>Chauliodus sloani</i>	Mesopelagic-Bathypelagic	Carnivore	La Pérouse	8, 9	2	139-153	146.1 ± 10.4			0.12 ± 0.01	
			MAD-Ridge	1	2	112-199	155.5 ± 61.4	10.9 ± 0.47	-18.9 ± 0.13	0.11 ± 0.01	4.1 ± 0.15
			MZC	20	2	121-202	161.8 ± 57.3	10.8 ± 1.1	-19.1 ± 0.38	0.11 ± 0.04	4.1 ± 0.34
<i>Diplophos taenia</i>	Mesopelagic	Carnivore	Reunion Is	3	1	184.9	184.9			0.10	
			MAD-Ridge	5	1	175.5	175.5	9.9	-18.9	0.21	3.8
<i>Echistoma barbatum</i>	Mesopelagic-Bathypelagic	Carnivore	MZC	21	2	82-115	98.5 ± 23.9	8.8 ± 0.57	-19.4 ± 0.16	0.08 ± 0.02	3.4 ± 0.18
			MAD-Ridge	9, 10, 11	5	68-81	72.3 ± 5.21	9.48 ± 1.11	-18.5 ± 0.30	0.15 ± 0.06	3.6 ± 0.35
<i>Eustomias</i> sp.	Mesopelagic-Bathypelagic	Carnivore	MZC	19	1	70.2	70.2	10.5	-18.5	0.12	4.0
			MZC	18	1	112.2	112.2	9.7	-18.5	0.06	3.7
<i>Idiacanthus fasciola</i>	Mesopelagic-Bathypelagic	Carnivore	La Pérouse	10	1	244.8	244.8	10.0	-17.7	0.12	3.5
<i>Melanostomias</i> sp.	Mesopelagic	Carnivore	La Pérouse	9	1	97.9	97.9	11.3	-18.0	0.17	3.9
			MAD-Ridge	5, 9	2	95	95.1 ± 0.29	9.81 ± 0.81	-18.1 ± 0.53	0.20 ± 0.07	3.7 ± 0.25
			MZC	20	1	118.0	118.0	11.1	-18.3	0.26	4.1
<i>Leptostomias</i> sp.			Reunion Is	3	1	131.4	131.4			0.26	
<i>Photonectes</i> sp.	Mesopelagic	Carnivore	La Pérouse	9, 10	2	117-126	121.1 ± 6.43	11.8 ± 0.62	-18.1 ± 0.62	0.22 ± 0.12	4.0 ± 0.19
<i>Photostomias</i> sp.	Mesopelagic	Carnivore	La Pérouse	9	1	110.8	110.8	11.1	-18.4	0.14	3.8
<i>Stomias boa</i>	Mesopelagic	Carnivore	La Pérouse	10	1	145.0	145.0	10.8	-18.4	0.13	3.7
<i>Stomias longibarbatu</i> s	Mesopelagic-Bathypelagic	Carnivore	MAD-Ridge	2	1	290	290	12.0	-18.3	0.38	4.4
			MZC	20	1	371	371.0	11.8	-18.6	0.90	4.4

Table 2. Minimum (Min), Maximum (Max) and mean \pm standard deviations of Hg concentrations ($\mu\text{g g}^{-1}$ dw) of the broad categories (crustaceans, fishes and squids) at La Pérouse, MAD-Ridge seamounts, the southern Mozambique Channel and Reunion Island.

Broad Category						
Region	Statistics	Crustaceans		Fishes		Squids
La Pérouse	Min	0.003	Oplophoridae	0.04	<i>D. perspicillatus</i>	0.05 <i>Abraliopsis</i>
	Max	1.69	Oplophoridae	0.48	<i>L. gemellarii</i>	0.08 <i>Abraliopsis</i>
	Mean \pm S.D.		0.40 \pm 0.41		0.19 \pm 0.11	0.06 \pm 0.01
MAD-Ridge	Min	0.05	<i>Funchalia</i>	0.03	<i>D. macarellus</i>	0.04 <i>O. volatilis</i>
	Max	0.71	Oplophoridae	1.12	<i>A. aculeatus</i>	0.26 <i>O. volatilis</i>
	Mean \pm S.D.		0.24 \pm 0.22		0.24 \pm 0.18	0.15 \pm 0.22
MZC	Min	0.06	<i>Funchalia</i>	0.03	<i>D. macarellus</i>	
	Max	0.27	Sergestidae	0.90	<i>S. longibarbus</i>	
	Mean \pm S.D.		0.15 \pm 0.08		0.18 \pm 0.18	
Reunion Island	Min	0.05	<i>Funchalia</i>	0.03	<i>D. macarellus</i>	0.02 <i>Onychoteuthis</i>
	Max	1.57	Oplophoridae	1.37	<i>S. elongatus</i>	0.19 <i>Abralia</i>
	Mean \pm S.D.		0.25 \pm 0.41		0.18 \pm 0.21	0.07 \pm 0.04